UNIVERSITY OF PADUA

Department of Pharmaceutical and Pharmacological Sciences

PhD SCHOOL IN BIOMEDICINE,
REGENERATIVE MEDICINE CURRICULUM
XXVIII° CYCLE

PhD Thesis

DESIGN AND DEVELOPMENT OF A POLYMERIC TUBULAR SCAFFOLD FOR PERIPHERAL NERVE REGENERATION

PhD School Director: **Prof. Stefano Piccolo**
Curriculum Coordinator: **Prof. Teresa Conconi**
Tutor: **Prof. Claudio Grandi**

PhD Student: **Dr. Lucia Lora**

Academic Year 2016-2017

INDEX

ABSTRACT

Peripheral nerve injury is a common clinical problem significantly affecting the patients' quality of life. In case of severe transections, the bridging of the gap between the proximal and distal nerve stumps is required and autologous nerve grafts using sensory nerves (i.e. the sural nerve or antebrachial cutaneous nerve) are the current criterion standard. Nevertheless, donor-site morbidities, permanent loss of function, size mismatch between the donor nerve and the injured nerve and poor functional recovery rates have prompted the interest towards the identification of an alternative to this technique.

To date, surgeons and researchers are turning their attention towards different grafts made of biological or artificial polymers. In fact, the development of hollow nerve guide conduits a) creating an adequate microenvironment for nutritional support/axons regeneration; b) acting as a barrier against the surrounding tissue infiltration; c) matching the effectiveness of the autologous nerve graft, would be beneficial to the field of peripheral nerve surgery.

Over the years, many biomaterials of natural or synthetic origin and with different characteristics in terms of biodegradability have been studied. However, it has not been identified yet a prosthesis able to guarantee a better regenerated tissue than the others.

The aim of the present study was to manufacture and investigate *in vitro* and *in vivo* the characteristics and the regenerative potential of three different nerve conduits made up of polyvinyl alcohol (PVA); 1% Oxidized PVA (1% Ox PVA) and Silk-Fibroin (SF). While the use of PVA and SF for the realization of neuro-guides has already been studied in the past, oxidized PVA (recently patented by our research group) is a new material for this purpose. In parallel, this study also allowed to assess the quality of axonal regeneration guaranteed by neuro-guides with different origin (synthetic vs natural) and biodegradation properties (non-biodegradable vs biodegradable).

After preparing the three different polymer solutions, disk-shaped and tubular supports were manufactured. These were employed for *in vitro* and *in vivo* studies respectively. Considering *in vitro* analysis, a morphological characterization of supports was performed by Scanning Electron Microscopy (SEM). Thereafter, the biocompatibility and the biological activity of the three different scaffolds was assessed using a Schwann-cell line (SH-SY5Y). Cells were seeded on supports and their adhesion and proliferation was evaluated by SEM and MTT assay at two different end-points (3 and 7 days from seeding). Regarding *in vivo* tests, nerve conduits were implanted in animal models (Sprague-Dawley rats) of peripheral nerve injury with loss of substance (nerve gap: 5 mm). At 12-weeks from surgery, the functional recovery of the sciatic nerve was assessed; thereafter, the animals were euthanized and the dissection occurred. Prior to explant, the gross appearance of grafts was carefully observed *in situ*. Specimens were than processed for histological (hematoxylin and eosin staining) and immunohistochemical analysis (anti-CD3; anti-S100) as well as for further Transmission Electron Microscopy (TEM) analysis. The objective was to assess the quality of the regenerated nerve-tissue highlighting any differences in efficacy between the three types of nerve-conduits; to this end, the histomorphological analysis has been fundamental allowing to quantify the axons (myelinated vs unmyelinated nerve fibers) at different levels of the explant (proximal vs central vs distal portion); the controlateral sciatic nerve was used as control.

Considering the *in vitro* results, SEM micrographs showed that PVA and SF supports have a smooth and regular surface; conversely, a certain roughness was noticed observing the ultrastructure of 1% Ox PVA disk-shaped scaffolds. Despite the superficial appearance of supports, it does not seem to affect the interaction with the cells. In fact, PVA-based scaffolds do not support cell adhesion and proliferation; SEM analysis and the MTT assay do not identified the presence of SH-SY5Y cells after 3 and 7 days from seeding. This result can be attributed to the high hydrophilic nature of the hydrogels. Conversely, SF scaffolds are adequate to promote SH-SY5Y cells growth.

Regarding the *in vivo* study, all nerve conduits showed good characteristics in terms of handiness, being easy-suturing and demonstrating also an adequate tear-resistance feature; PVA-based scaffolds appear more flexible than SF guides. After 12 weeks from surgery, all animals showed a sciatic nerve functional recovery; in particular, all of them supported their body weight on the hind leg even though animals implanted with PVA and SF nerve conduits sometimes showed spasms during the walk while not limping. On the contrary, animals implanted with 1% Ox PVA nerve conduits exhibited a normal movement. At the time of dissection, the three scaffolds were still clearly identifiable. Any dislocation of the grafts or neuroma formation at the stumps was observed; moreover, the transparency of the three scaffolds allowed to identify the presence of a regenerated tissue inside. Thereafter, histological and immunohistochemical analysis were performed to evaluate the quality of axonal regeneration. Preliminarily, the haematoxylin and eosin staining of the specimens (cross-section of the central portion) highlighted the morphological integrity of the structure. In fact, three layers are recognizable proceeding from the periphery to the inside of the sections: an external fibrous capsule; a layer corresponding to the nerve conduit; a homogeneous and dense regenerated tissue in the middle. The biocompatibility of the *grafts* was verified by immunohistochemical analysis; anti-CD3 immunohistochemistry demonstrated the absence of severe inflammatory reactions. At the same time, several $S100^+$ cells were identified suggesting the extensive presence of Schwann-cells.

In parallel, the typical peripheral nerve morphology was highlighted also by Toluidine Blue staining, both in the proximal and distal stumps. Although all samples support the recovery of the lesion, some differences can be found between the three experimental groups; these results were confirmed also by TEM micrographs.

The histomorphometric analysis of samples evaluated the total axons number per nerve and axon density (axons/μm^2); for each graft were considered the proximal, the central and the distal section. The collected data showed that 1% Ox PVA conduits assure a better outcome in nerve

regeneration than the non-biodegradable PVA grafts which among the three groups proved to be the ones with the lower outcomes.

The results of this study showed that all nerve conduits considered (PVA; 1% Ox PVA and SF) promote peripheral nerve regeneration in case of neurotmesis with loss of substance. Considering the quality of regenerates, better outcomes were observed analyzing the 1% Ox PVA explants compared to PVA and Silk-Fibroin ones.

RIASSUNTO

Le lesioni nervose periferiche costituiscono un problema clinico piuttosto comune, il quale inficia in modo significativo la qualità della vita dei pazienti. In caso di lesioni gravi con perdita di sostanza, al fine di colmare il gap tra il moncone prossimale ed il distale, il *gold-standard* prevede l'impianto di innesti nervosi autologhi utilizzando nervi sensoriali (ad es., nervo surale o nervo cutaneo antibrachiale). Tuttavia, criticità quali la morbidità del sito donatore, la perdita in funzionalità, la mancata corrispondenza dimensionale tra il nervo donatore ed il nervo lesionato oltre ad uno scarso recupero funzionale hanno spinto l'interesse verso l'identificazione di un approccio alternativo.

Allo stato dell'arte, chirurghi e ricercatori stanno volgendo la loro attenzione verso innesti polimerici diversi (*grafts*) di natura sia biologica che artificiale. Infatti, lo sviluppo di neuroguide capaci di: a) creare un microambiente ideale per la rigenerazione assonale; b) fornire una protezione dall'infiltrazione di tessuto circostante; c) possedere un'efficacia analoga a quella garantita dall'innesto nervoso autologo; costituirebbe un vantaggio significativo nell'ambito della chirurgia del nervo periferico.

Nel corso degli anni, sono stati studiati molti biomateriali di origine sia naturale che sintetica aventi caratteristiche differenti in termini di biodegradabilità. Tuttavia, considerando la qualità del tessuto rigenerato, non è ancora stata individuata una protesi più performante rispetto alle altre.

L'obiettivo di questo studio è stato quello di allestire e studiare, sia *in vitro* che *in vivo,* le caratteristiche ed il potenziale rigenerativo di tre diverse neuroguide rispettivamente costituite da: alcool polivinilico (PVA); PVA ossidato 1% (PVA Ox 1%) e Fibroina della Seta (FS). Mentre l'impiego di PVA e FS per la realizzazione di *grafts* è già stato investigato in passato, il PVA Ox 1% (recentemente brevettato dal nostro gruppo di ricerca) costituisce un nuovo materiale per questo scopo. In parallelo, questo studio ha anche consentito di confrontare la

qualità della rigenerazione assonale sostenuta da neuroguide diverse sia per origine (sintetica vs naturale) che per proprietà biodegradative (biodegradabili vs nonbiodegradabili).

Dopo aver allestito le tre diverse soluzioni polimeriche, sono stati quindi preparati *scaffolds* sia discoidali che in forma di *graft* tubulare, utilizzati rispettivamente per i successivi studi *in vitro* e *in vivo*. Nell'ambito degli studi *in vitro*, è stata effettuata una caratterizzazione morfologica dei supporti mediante microscopia elettronica a scansione (SEM). Successivamente, la biocompatibilità e l'attività biologica dei tre differenti *scaffolds* è stata valutata utilizzando una linea di cellule di Schwann (SH-SY5Y). Le cellule sono state seminate sui supporti e la loro adesione e la proliferazione è stata valutata mediante saggio MTT oltre che SEM a due differenti *end-point* (3 e 7 giorni dalla semina). Per quanto riguarda lo studio *in vivo*, i *graft* tubulari sono stati impiantati in modelli animali (ratti Sprague-Dawley) di lesione nervosa periferica con perdita di sostanza (gap tra moncone prossimale e distale: 5 mm). A 12 settimane dalla chirurgia, è stato valutato il recupero funzionale del nervo sciatico; successivamente, gli animali sono stati sacrificati. Dopo dissezione, prima di procedere all'espianto, l'aspetto macroscopico degli innesti è stato attentamente osservato *in situ*. I campioni sono stati quindi prelevati e trattati per le successive analisi istologiche (ematossilina ed eosina) ed immunoistochimiche (anti-CD3; anti-S100) nonché per ulteriori analisi di microscopia elettronica a scansione (TEM). L'obiettivo è stato quello di valutare la qualità del tessuto rigenerato evidenziando eventuali differenze di efficacia tra i tre tipi di *grafts*; a tal fine, anche l'analisi istomorfologica si è rivelata fondamentale, permettendo di quantificare gli assoni (mielinici vs amielinici) in diverse porzioni del campione (porzione prossimale vs centrale vs distale). Il nervo sciatico controlaterale è stato usato come controllo.

Considerando i risultati degli studi *in vitro*, le immagini al SEM hanno mostrato come i supporti in PVA e FS mostrino una superficie liscia e regolare; al contrario, una certa ruvidità è stata notata osservando l'ultrastruttura degli *scaffold* discoidali in PVA Ox 1%. Nonostante il diverso aspetto ultrastrutturale dei supporti, esso non sembra influenzare l'interazione con le cellule. Il

PVA (sia nativo che ossidato) non sostiene l'adesione e la proliferazione cellulare; infatti, sia le analisi al SEM che il saggio MTT non hanno identificato la presenza di cellule SH-SY5Y dopo 3 e 7 giorni dalla semina. Questo risultato può essere attribuito alla elevata idrofilia degli idrogeli, al contrario, gli *scaffold* in FS sono adeguati per promuovere la crescita delle SH-SY5Y.

Per quanto riguarda lo studio *in vivo*, tutti i *graft* mostrato buone caratteristiche in termini di manipolabilità, essendo facilmente suturabili e dimostrando anche una adeguata resistenza allo strappo; gli *scaffold* in PVA appaiono più flessibili rispetto alle guide in FS. Dopo 12 settimane dalla chirurgia, tutti gli animali hanno mostrato un certo recupero funzionale dell'arto operato; in particolare, tutti distribuivano il proprio peso corporeo anche sulla zampa posteriore. Pur non zoppicando, gli animali impiantati con PVA e SF mostravano talvolta degli spasmi durante la deambulazione, al contrario, gli animali impiantati con *graft* in PVA Ox 1% esibivano un movimento normale. Al momento della dissezione, i tre *graft* erano ancora chiaramente identificabili. Non è stata riscontrata alcuna dislocazione degli innesti o formazione di neuroma in corrispondenza dei monconi; inoltre, la trasparenza delle tre neuroguide ha permesso di identificare la presenza di un tessuto rigenerato al loro interno. Successivamente, sono state effettuate analisi istologiche ed immunoistochimiche per valutare la qualità della rigenerazione assonale. Preliminarmente, mediante colorazione con ematossilina ed eosina (sezione trasversale della porzione centrale) è stato possibile mettere in evidenza l'integrità morfologica della struttura. Procedendo dalla periferia della sezione verso l'interno sono riconoscibili: una capsula fibrosa esterna, il *graft* ed il tessuto neo-rigenerato, omogeneo e denso, nel mezzo. La biocompatibilità degli innesti è stata verificata mediante analisi immunoistochimica; la scarsa presenza di cellule $CD3^+$ ha dimostrato l'assenza di reazioni infiammatorie gravi riconducibili all'impianto. Contestualmente, l'elevata presenza di elementi $S100^+$ riscontrata in tutti i campioni ha comprovato una evidente rigenerazione assonale.

In parallelo, la morfologia tipica del tessuto nervoso periferico è stata altresì evidenziata mediante colorazione con Blu di Toluidina mediante la quale è stato considerato anche l'aspetto dei monconi prossimale e distale.

Sebbene tutti i campioni supportino il recupero della lesione, alcune differenze possono essere riscontrate tra i tre gruppi sperimentali; questi risultati sono stati confermati anche dalle micrografie al TEM. L'analisi morfometrica dei campioni ha valutato il numero totale di assoni/nervo e la loro densità (assoni / μm^2); per ogni innesto sono state considerate le sezioni prossimale, centrale e distale. I dati raccolti hanno dimostrato che il PVA Ox 1% assicura un risultato migliore nella rigenerazione assonale rispetto agli innesti non biodegradabili in PVA, il quale tra i tre gruppi è risultato essere quello con l'outcome inferiore.

I risultati di questo studio hanno mostrato che, in caso di neurotmesi con perdita di sostanza, tutti i *graft* allestiti (PVA; PVA Ox 1% e FS) promuovono la rigenerazione del nervo. Considerando la qualità del tessuto rigenerato, sono stati osservati dei risultati migliori con *graft* in PVA Ox 1% rispetto a quelli ottenuti da neuroguide in PVA e FS.

INTRODUCTION

1. Peripheral nerve injuries: a global clinical problem

Peripheral nerve injury (PNI) is a common global clinical problem significantly affecting the patients' quality of life and causing enormous socio-economic burdens (Gu et al., 2014).

PNI afflicts 2.8% of trauma patients annually. There are around 360,000 cases of upper extremity paralytic syndromes in the United States and more than 300,000 peripheral nerve injuries in Europe on an annual basis (X. Wang et al., 2014). In head and neck surgery, PNI frequently involves the facial nerve, being peripheral facial paralysis the most common pathology of the cranial nerves. Its incidence ranges from 20 to 30 cases per 100,000 people (Gaudin et al., 2016).

It is possible to distinguish between a primary and a secondary injury of a peripheral nerve. Primary injury commonly results from the same trauma that damages a bone or joint; eventhough, it can be caused also by the displacement of osseous fragments, stretching, manipulation, rather than by the initial injuring force. Secondary injury results from infections, scars, callus, or vascular complications including hematoma, arteriovenous stula, ischemia, or aneurysm. Less commonly, peripheral nerves can also be injured by metabolic or collagen diseases, malignancies, endogenous or exogenous toxins, or thermal/chemical trauma (Jobe et al., 2016).

Compromising neuronal communication along sensory/motor nerves between the central nervous system (CNS) and the peripheral organs, PNJs can potentially lead to lifelong disabilities. Although the peripheral nervous system (PNS) has a greater capacity for axonal regeneration after injury, spontaneous peripheral nerve repair is nearly always incomplete with poor functional recovery ([a]Arslantunali et al., 2014; X. Wang et al., 2014). Various types of medical therapy have been undertaken for several hundred years with the intention of improving outcomes (Gu et al., 2014). Up to now, epineural repair is the most appropriate surgical

procedure when there is a small gap between the nerve endings. Conversely, if the distance between the stumps of the nerve is significant, repairing a transected nerve is very difficult or impossible without a graft or a conduit tube (Mohammadi et al., 2016).

Current research focusing on pharmacological agents, immune system modulation, enhancing factors, and entubulation chambers, although promising, so far have had little clinical application, and the results of nerve repair remain modest with only 50% of patients regaining useful function (Jobe et al., 2016).

2. The Peripheral Nervous System

The nervous system is structurally and functionally the most complicated organ of the human body (Trapp et al., 2017). It is possible to distinguish between the: a) central nervous system, consisting of the brain and the spinal cord; b) peripheral nervous system which encompass all cranial, motor, sensory, and autonomic nerves that extend outside the dural confines of the brain and spinal cord (L. Chen et al., 2017) and conduct impulses from and to the CNS ([a]Arslantunali et al., 2014).

2.1. Organization of the Peripheral Nervous System

In the PNS it is possible to recognize:

- *Motor somatic fibers*. They have their cell bodies within the ventral horn of the spinal cord and extend axons that travel through the ventral root and eventually form motor end plates at the neuromuscular junction of the skeletal muscles (K. S. Chen et al., 2017; Jobe et al., 2016).

- *Sensory somatic fibers*. They arise from pain, thermal, tactile, stretch receptors (Jobe et al., 2016) and proprioception (Drake et al., 2014) and extend to their cell bodies, the dorsal root ganglia, which lie within the bony intervertebral foramen. These sensory fibers make up the dorsal (posterior) rootlets that enter the posterior horn of the spinal cord (Tsao et al., 2016).

- *The autonomic component* of all mixed spinal nerves leaves the spinal cord along only 14 motor roots (Jobe et al., 2016). Sympathetic preganglionic neurons are located in the intermediolateral horn of the thoracic and upper lumbar spinal cord and synapse in the paraspinal sympathetic trunk or along splanchnic ganglia, which in turn send axons to target organs. Parasympathetic preganglionic neurons, on the other hand, are located within the brainstem and send axons that synapse on ganglia closely associated with target organs (K. S. Chen et al., 2017) (Figure 1).

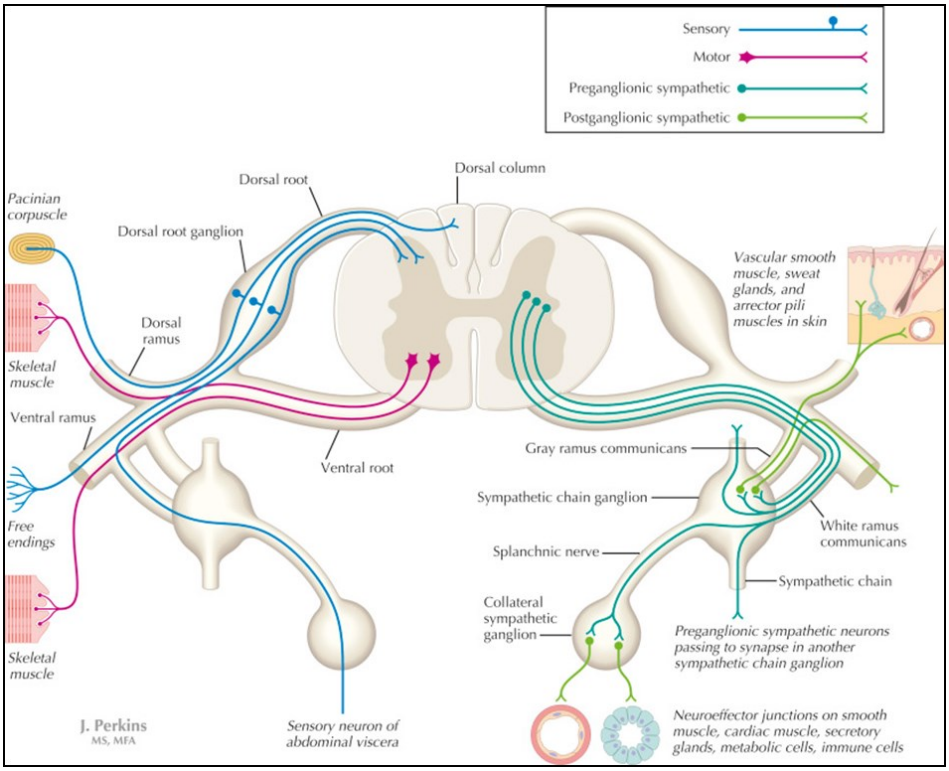

Figure 1. Peripheral nerves anatomy. Sensory, motor and autonomic components (Felten et al., 2016).

Leaving the intervertebral foramina, all these fibers bundle in the peripheral nerves (Felten et al., 2016). A total of 31 nerves exit on each side of the spine to innervate the homolateral trunk and extremities: 8 cervical, 12 thoracic, 5 lumbar, 5 sacral, and one coccygeal (Jobe et al., 2016).

Then peripheral nerves promptly branch into anterior and posterior primary rami. The posterior primary rami are directed posteriorly and supply the paraspinal musculature and the skin along the posterior aspect of the trunk, the neck, and the head. Anterior primary rami of all the cervical, the first thoracic, and all the lumbosacral nerves join in the formation of plexuses: cervical, brachial, lumbar and lumbosacral, thus losing the primitive myomeric pattern. All the other thoracic rami retain their autonomy and supply one intercostal dermatomal and myotomal segment (Jobe et al., 2016).

2.2. Microscopic anatomy of peripheral nerves

On microscopic view, the nerve fiber is the axon in association with its enveloping Schwann cells, which form myelin in some types of fibers (L. Chen et al., 2017). Schwann cells have a complex homeostatic relationship with the axon, and they also play a critical role, together with the basal lamina, in nerve regeneration (Cederna et al., 2009).

Sensory and motor nerves contain unmyelinated and myelinated fibers in a ratio of 4:1. In the unmyelinated or sparsely myelinated fibers, several axons are wrapped by a single Schwann cell. In the more heavily myelinated fibers, the Schwann cell by rotation forms a multilaminated structure that encloses a myelin sheath around a single axon. The segment of myelinated nerve fiber enclosed by a single Schwann cell is referred to as an internode and varies in length from 0.1 to 1.8 mm, with the more heavily myelinated fibers having the longer internodes. The point at which one Schwann cell ends and the next begins is relatively sparse in myelin and is called the nodal gap, or node of Ranvier (Jobe et al., 2016) (Figure 2).

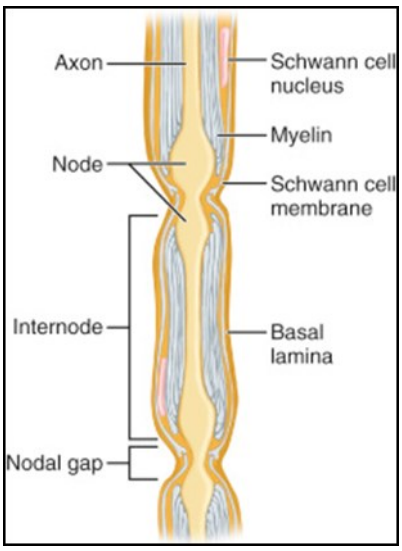

Figure 2. Basic anatomy of a myelinated nerve fiber (Jobe et al., 2016).

The node of Ranvier is the site on the membrane where sodium channels are present and is also the site of initiation or reinitiation of the action potential (Felten et al., 2016). Conduction of these axon potentials along the nerve is the means by which information is transmitted between the cell body and the processes at the end of the axon extensions (Heath et al., 1998).

A peripheral nerve is therefore composed of unmyelinated and myelinated axons; the connective sheaths with which they are associated; and local blood vessels, the vasa nervorum (Felten et al., 2016). The connective tissue accounts for 30% to 75% of the nerve's cross-sectional area and conduct a fundamental role in the nerve repairing process. The connective tissue components include the endoneurium, perineurium, and epineurium (Cederna et al., 2009).

The endoneurium is a veil of delicate fibrous tissue surrounding the axon with its Schwann cell and myelin sheath. Seen longitudinally, the endoneurium forms a tube encircling individually the Schwann cell sheaths that cluster together to form a fascicle (or funicle as termed by Sunderland) (Jobe et al., 2016), which is the smallest structural unit that can be subjected to surgical suture (L. Chen et al., 2017). Perineurium surrounds individual fascicles. It has stronger tensile strength than does epineurium. The elastic property of the nerve under elongation is

preserved as long as the perineurium keeps intact. However, if the nerve trunk is stretched by 20% of its length, which exceeds the tensile strength of the perineurium, the nerve is almost certain to suffer a discontinuity (L. Chen et al., 2017).

Perineurium functions as a blood-nerve barrier and helps to protect the axons from local diffusion of potentially damaging substances (Felten et al., 2016) and damage to this structure induces loss of homeostasis of the nerve. For this reason, the surgeon who is performing decompression should exercise great care not to breach the perineurium (L. Chen et al., 2017).

The number of fascicles in a nerve varies from 1 to more than 100, with the diameter mostly ranging from 0.04 to 2 mm. Studies have shown that although the fascicular arrangement is complex in the proximal aspect of a peripheral nerve, the distal fascicles can be dissected over long distances before merging occurs. This characteristic is important to the surgeon when intraneural dissection is required for accurate neurorrhaphy (Jobe et al., 2016).

The epineurium consists of loose collagenous connective tissue that either encloses groups of nerve fascicles (external epineurium) or cushions fascicles from external pressure and trauma to prevent injury (internal epineurium). The amount of external and internal epineurium varies greatly among individuals, peripheral nerves, and even within a single nerve (Cederna et al., 2009) (Figure 3).

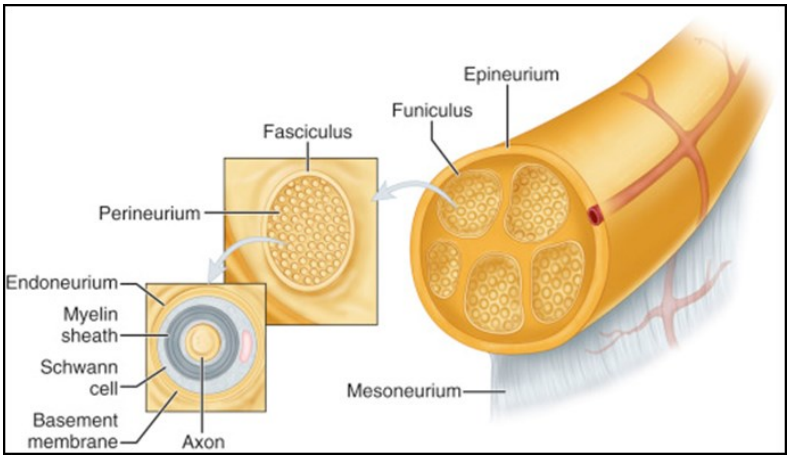

Figure 3. Basic anatomy of peripheral nerves (Jobe, 2017).

Each nerve has a vascular network along its entire length including arteries, veins, and capillaries (Cederna et al., 2009). There is an extrinsic (segmental) and an intrinsic (longitudinal) blood supply to each nerve. The intrinsic blood supply that runs longitudinally within the epineurium, perineurium, and endoneurium is fairly extensive and allows surgical mobilization without complete devascularization over variable lengths of nerves (Jobe et al., 2016). As mentioned, these vascular components of the peripheral nerve are anatomically separated from the neural components of the nerve by the blood–brain barrier (Cederna et al., 2009).

3. Peripheral nerve injuries

3.1. Physiopathology of nerve injuries

Mature neurons (like many other cells in the body) do not replicate; that is, they do not undergo cell division. Instead, under the right conditions, axon extensions in the PNS can regenerate over gaps caused by injury, reconnecting with the distal stump and eventually reestablishing functional contacts (Heath et al., 1998). However, the spontaneous regeneration is often incomplete, and in turn this can lead to neuropathic conditions. Therefore, there is a great deal of interest in elucidating different factors involved in PNS regeneration, and how they regulate regeneration in injured nerves (L. Chen et al., 2017).

Following traumatic injury to peripheral nerves, a series of pathophysiological events occurs in the injured nerve, leading to axon degeneration back to the adjacent node of Ranvier in the proximal stump (or primary, traumatic, or retrograde degeneration) and Wallerian (or secondary) degeneration in the distal stump (Gu et al., 2014), which are histologically identical (Jobe et al., 2016). This process results in the breaking up and dissolution of the peripheral axon (Felten et al., 2016) and further extends beyond the axon to the Schwann cell envelope and myelin sheath, to the cell body, and ultimately, to the motor and sensory end-organs (Birch,

2011) (Figure 4). Adjacent uninjured fibers are exposed to a dramatically altered endoneurial environment (Ringkamp et al., 2013).

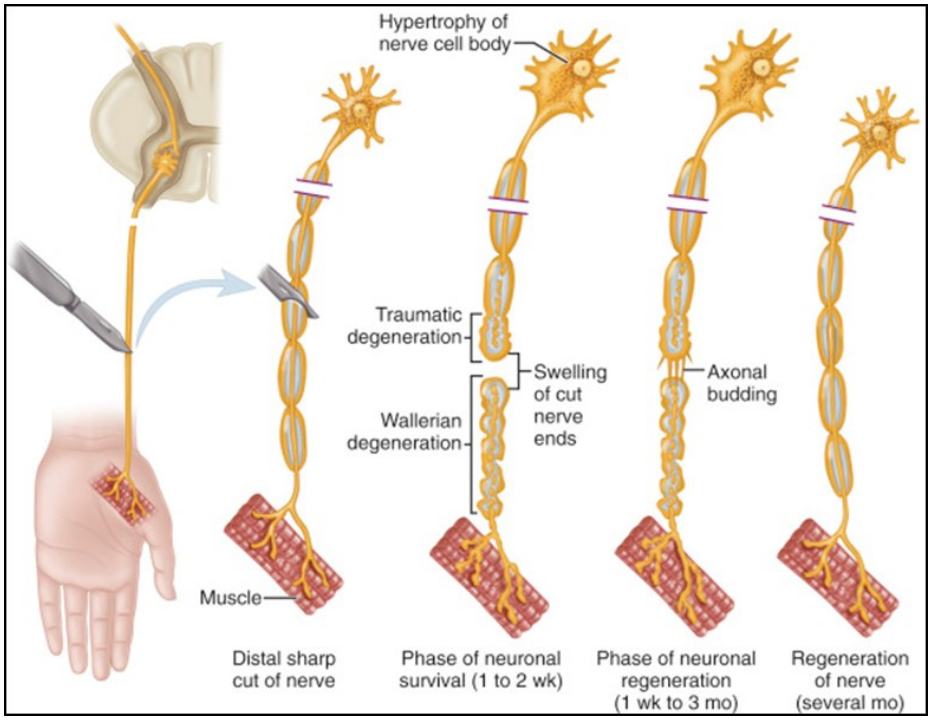

Figure 4. Physiologic changes of peripheral nerve axon after traumatic injury (Jobe et al., 2016).

The time required for degeneration varies between sensory and motor segments and is related to the size and myelinization of the fiber (Jobe et al., 2016). Although very proximal injury may lead to apoptosis of the cell body itself, the more common consequence of axonal injury is for the cell body to go through the process of chromatolysis (Tsao et al., 2016). The Nissl bodies (endoplasmic reticulum) break up into individual ribosomes, the cell body swells, and the neuron shifts its metabolism to structural and reparative synthetic products that attempt to save the neuron and permit it to try to recover from the injury. If successful, this process gradually reverses, and the neuron begins to sprout a peripheral axonal extension, seeking to reattach to the target from which it was disrupted (Felten et al., 2016). If not successful, dissolution of the cell body occurs. Cell loss is more severe in more proximal axonotomy and it is more severe in the neonate than in the adult (Birch, 2011). Chromatolysis is evident by day 7, and death or

evidence of beginning recovery is apparent after 4 to 6 weeks. With recovery, the edema begins to subside, the nucleus migrates toward the center of the cell, and Nissl substance begins to reaccumulate (Jobe et al., 2016).

Wallerian degeneration is a complicated process that is initiated following metabolic or mechanical damage to peripheral nerves and that induces multiple changes including axonal degeneration, myelin breakdown, glial cell proliferation, blood–nerve barrier compromise, as well as the infiltration and activation of macrophages (L. Chen et al., 2017). Distal axon injury leads to disruption of retrograde and anterograde flow of signals within the axon (Tsao et al., 2016) and subsequently conduction is lost (Birch, 2011). The entire axonal process of Wallerian degeneration takes approximately 1 week (Tsao et al., 2016). During the first 3 days after injury, definite morphologic changes become apparent in the axon (L. Chen et al., 2017). Rapid inflow of extracellular ions such as calcium and sodium occurs through the disruption in the axonal plasma membrane, which activates a cascade of events that shares features with programmed cell death or apoptosis (Tsao et al., 2016). After 2 or 3 days, the distal segment becomes fragmented, and with subsequent fluid loss the fragments begin to shrink and to assume a more oval or globular appearance. A concomitant fragmentation and shrinkage of the myelin sheath parallels the axonal degenerative change (Jobe et al., 2016). However, PNS is not completely isolated, and the injured axons trigger a complex multi-cellular response that involves multiple components. In addition to cellular responses elicited by injured axons, Wallerian degeneration is accompanied by the de-differentiation of Schwann cells and activation of immune response. Schwann cells play an important role in the early stage of Wallerian degeneration. Upon injury, Schwann cells begin to dedifferentiate in the distal nerve depending on the ubiquitin–proteasome system, a process that alters the gene expression profile of Schwann cells and provides an environment for axonal degeneration (L. Chen et al., 2017). Therefore, activated Schwann cells begin to digest myelin (Tsao et al., 2016) and axonal debris until empty endoneurial tubes remain (L. Chen et al., 2017). The collapsed columns of Schwann

cells have a characteristic band-like appearance under electron microscopy; these columns are known as the bands of Büngner, and provide a pathway along which new axons are destined to grow (Weber et al., 2010). This supportive environment is critical for successful axonal regeneration (Grinsell et al., 2014).

In the later stages of Wallerian degeneration, macrophages are the major cells contributing to remove myelin and axonal debris. The infiltration of macrophages into injured nerves is overtly seen starting from 2 to 3 days and peaking at 7 days post-injury. Upon the migration from the vasculature into tissues, under the specific local microenvironment education, monocytes can differentiate into distinct populations of macrophage, with distinct functional profile. In the peripheral nerve injured site it has been shown that macrophages can be divided into "classically activated" pro-inflammatory phenotype (M1) and "alternatively activated" anti- inflammatory phenotype (M2). M1 macrophages are the effector and inducer cells in pro-inflammatory responses, and they are activated by lipopolysaccharide (LPS), interferon gamma (IFN-γ) and/or tumor necrosis factor alpha (TNF- α). In contrast, M2 macrophages are involved in anti-inflammatory responses and activated by exposure to specific cytokines and factors, including IL-4, IL-13, IL-10, immune complexes, hormones or adenosine A2A receptors (A2AR) agonist. In general, M1 macrophages activate immune responses, whereas M2 macrophages are immunosuppressive cells that promote tissue remodeling and repair, thus exhibiting a pivotal role in axonal regeneration (P. Chen et al., 2015).

By the third week after injury, scar tissue become evident as the fibroblasts deposit endoneurial collagen. As time passes, more and more collagen is deposited and the number of macrophages and Schwann cells decreases, and these change their phenotype to one less receptive to regenerating axons. Although these changes occur at varying intervals according to the nature of the injury, the evidence from the cellular and molecular responses suggests that the peak of "receptivity" to regenerating axons in the distal segment lies between 1 and 3 weeks after injury (Birch, 2011).

3.2. Effects of peripheral nerve injuries

Motor. When a peripheral nerve is severed at a given level, all motor function of the nerve distal to that level is abolished. All muscles supplied by branches of the nerve distal to that level are paralyzed and become atonic. Atrophy of muscle bulk progresses rapidly to 50% to 70% at the end of about 2 months. Atrophy continues at a much slower rate, and the connective tissue component of the muscles increases. Striations and motor endplate configurations are retained for longer than 12 months, whereas the empty endoneurial tubes shrink to about one third their normal diameter. Complete disruption and replacement of muscle fibers may not become complete until after 3 years (Jobe et al., 2016).

When the denervated muscle is replaced with scarring permanent functional deficits are present, even if the muscle becomes reinnervated. Optimal muscle function can therefore be expected if the muscle can become reinnervated within 1–3 months. However, even under these ideal circumstances, a force deficit in the reinnervated muscle may result. As the time period increases between denervation and reinnervation, the functional recovery declines. Reasonable recovery of skeletal muscle contractile function can be realized if the muscle is reinnervated within 12 months of denervation. After 2 years of denervation, little to no recovery of motor function can be expected (Cederna et al., 2009).

Sensory. Sensory loss usually follows a definite anatomical pattern, although the factor of overlap from adjacent nerves may confuse inexperienced surgeons. After severance of a peripheral nerve, only a small area of complete sensory loss is found. This area is supplied exclusively by the severed nerve and is called the autonomous zone or isolated zone of supply for that nerve. A larger area of tactile and thermal anesthesia is readily delineated and corresponds more closely to the gross anatomical distribution of the nerve; this larger area is known as the intermediate zone. When a nerve is intact, and the adjacent nerves are blocked or sectioned, an area of sensibility exceeds the gross anatomical distribution of the nerve; this area is known as the maximal zone.

It has long been recognized that the autonomous zone becomes smaller during the first few days or weeks after injury, long before regeneration is possible. Livingston suggested that this is caused by ingrowth of adjacent nerves, but resumption of or increase in function in anastomotic branches from adjacent nerves is a more plausible explanation. This decrease in the area of sensory loss might be interpreted by an inexperienced surgeon as evidence of regeneration or of incomplete injury and might be responsible for needless delay in exploration of the nerve (Jobe et al., 2016).

Reflex. Complete severance of a peripheral nerve abolishes all reflex activity transmitted by that nerve. This is true in severance both of the afferent or the efferent arc. Commonly, however, reflex activity is abolished in partial nerve injuries when neither arc is completely interrupted and is not a reliable guide to the severity of injury (Jobe et al., 2016).

Autonomic. Interruption of a peripheral nerve is followed by loss of sweating and of pilomotor response and by vasomotor paralysis in the autonomous zone. The area of anhidrosis usually corresponds to, but may be slightly larger than, the sensory deficit. If the injury is incomplete, and especially if it is associated with causalgia, sweating may be excessive and may involve areas beyond the intermediate zone of the nerve. Vasodilation occurs in complete lesions, and the area affected is at first warmer and pinker than the rest of the limb. After 2 to 3 weeks, however, the affected area becomes colder than the adjacent normal areas and the skin may be pale, cyanotic, or mottled in an area often extending beyond the maximal zone of the injured nerve. Trophic changes occur commonly and are most evident in the hands and feet. The skin becomes thin and glistening and, when subjected to trauma that ordinarily does little harm, breaks down to form ulcers that heal slowly. The fingernails become distorted, are often ridged or brittle, and may be lost entirely (Jobe et al., 2016).

3.3. Peripheral nerve regeneration

Within the first 24 hours after injury, axonal regeneration occurs; as many as 50–100 nodal sprouts appear and mature into a growth cone elongating in response to signals from local tissue and denervated motor and sensory receptors (neurotropic factors) (Grinsell et al., 2014). All axonal sprouts are initially unmyelinated whether they arise from a myelinated or an unmyelinated fiber (Jobe et al., 2016). Also proteases are released from the growth cone to aid axonal regeneration through tissue.

Axons regenerate as if they are influenced by certain neurotrophic substances contained within distal nerve tissue (Jobe et al., 2016) which attract or repulse the growth cone and prevent misdirected growth of axon sprouts (Tsao et al., 2016). Axonal sprouts grow from the proximal to the distal stump at a rate of approximately 1 to 2 mm/day, depending on the location of the lesion; with proximal lesions, growth may be as fast as 2 to 3 mm/day, while in distal lesions it is about of 1 mm/day (Tsao et al., 2016). In case of a critical gap (2 mm), the neurotrophic effect is almost absent; hence, minimizing the distance and the misalignment of the two nerve ends is paramount (Jobe et al., 2016).

Schwann cells play a key role in neuronal regeneration as they dedifferentiate and upregulate the expression of adhesion molecules and neurotrophins (i.e. cadherins, immunoglobulin superfamily factors, laminin) which promote the migration of nerve sprouts that form at the regenerating axon tip (Tsao et al., 2016). Moreover, the Schwann cells proliferate and generate new myelin sheaths around the regrowing axon that is thinner than the native one; thus, the regenerated axon shows a slower conduction velocity than the original intact axon (Felten et al., 2016).

The continuity of the endoneurial tube plays a fundamental role in alignment and containment of the regeneration process. As a matter of fact, an injury severe enough to interrupt the endoneurial tube can lead to axonal sprouts migrating aimlessly throughout the damaged area

into the epineurial, perineurial, or adjacent regions. These disorganized sprouts can form into a stump neuroma or neuroma in continuity, which can manifest clinically as a painful lump.

Moreover, when different tubes are damaged, axonal sprouts, barred from their endoneurial tube by scar tissue, might enter empty endoneurial tubes of other injured funiculi or regenerate through newly formed endoneurial tubes, thus terminating in myotomal or dermatomal areas other than their own (Jobe et al., 2016). The more severe an injury is, the more disordered the nerve regenerates, resulting in less axons reaching the distal sensory or motor target (Grinsell et al., 2014).

Therefore, lesser injuries without disruption of the endoneurial and Schwann cell sheaths are associated with excellent or acceptable anatomical regeneration. Conversely, more extensive injuries with complete disruption of the entire nerve, with wide separation of the ends of the nerve, and with the regenerating fibers obstructed by extensive scar tissue result in little or no return of function (Grinsell et al., 2014).

3.4. Classification of peripheral nerve injuries

According to Seddon (1943) nerve injuries can be classified into three pathologic types on the basis of the injury's locations: the axon, the myelin sheath, or the supporting connective tissue structures (endoneurium, perineurium, epineurium) (Rubin et al., 2010; Sonabend et al., 2012). These three types are defined as follows:

1. Neurapraxia, designating minor contusion or compression of a peripheral nerve with preservation of the axis-cylinder but with possibly minor edema or breakdown of a localized segment of myelin sheath. Transmission of impulses is physiologically interrupted for a time (Jobe et al., 2016), but prognosis for complete and spontaneous recovery is excellent within a 6-week period. Indeed, many patients return to normal within hours (Tsao et al., 2016).

2. Axonotmesis, designating more significant injury with breakdown of the axon and distal wallerian degeneration but with preservation of the epineurium, perineurium, and endoneurium. Complete distal wallerian degeneration occurs (Jobe et al., 2016). A preserved endoneurium implies that once the remnants of the degenerated nerve have been removed by phagocytosis, the regenerating axon simply has to follow its original course directly back to the appropriate end organ (Dillingham et al., 2016). Spontaneous regeneration occurs at a rate of 1 mm per day (Sonabend et al., 2012) and good functional recovery can be expected.

3. Neurotmesis, designating a more severe injury with complete anatomical severance of the nerve. This is complete disruption of the axon and all supporting connective tissue structures, whereby the endoneurium, perineurium, and epineurium are no longer in continuity. This lesion has a poor prognosis for complete functional recovery (Dillingham et al., 2016) without surgical intervention.

A more useful and readily applicable in clinical practice classification was described by Sunderland in 1951. According to this classification, peripheral nerve injuries are arranged in ascending order of severity from the first to the fifth degree, with each degree of injury suggesting a greater anatomical disruption and its correspondingly worse prognosis. Anatomically, the various degrees of injury represent injury to: myelin (Grade I), axon (Grade II), the endoneurial tube and its contents (Grade III), perineurium (Grade IV), and the entire nerve trunk (Grade V) (Jobe et al., 2016). The most important goal of Sunderland's work was to clarify the classification proposed by Seddon (Roberts et al., 2015).

In first-degree injury, conduction along the axon is physiologically interrupted at the site of injury but the axon is not disrupted. No Wallerian degeneration occurs, and recovery is spontaneous and usually complete within a few days or weeks (Jobe et al., 2016). This injury is similar to Seddon’s neurapraxia (Roberts et al., 2015). The loss of function varies. Usually, motor function is more profoundly affected than sensory function. Sensory modalities are

affected in order of decreasing frequency as follows: proprioception, touch, temperature, and pain. Sympathetic fibers are the most resistant to this type of injury. If sensory modalities are markedly affected, paresthesias may be present for several days. If they are disturbed at all, sympathetic function often returns promptly; the modalities of pain and temperature also are commonly preserved or return promptly. Proprioception and motor function usually are the last to return (Sonabend et al., 2012).

In second-degree injury, disruption of the axon is evident (Jobe et al., 2016) as in Seddon's axonotmesis. There is no disruption of the axon sheaths, endoneurium, or perineurium, and other supporting structures remain intact (Sonabend et al., 2012), providing a perfect anatomical course for regeneration (Jobe et al., 2016).

Wallerian degeneration distal to the point of injury and degeneration proximal for one or more nodal segments occur. Clinically, the neurological deficit is complete with loss of motor, sensory, and sympathetic function (Jobe et al., 2016). During regeneration, the nerve fiber pattern remains the same, ensuring complete restoration of function (Sonabend et al., 2012).

In third-degree injury, the axons and endoneurial tubes are disrupted but the perineurium is preserved. The result is disorganization resulting from disruption of the endoneurial tubes. Scar tissue within the endoneurium can obstruct certain tubes and divert sprouts to paths other than their own. Clinically, the neurological loss is complete in most instances, and because of the additional time required for the regenerating axon tips to penetrate the fibrous barrier, the duration of loss is more prolonged than in second-degree injury. Returning motor function is evident from proximal to distal, but with varying degrees of permanent motor or sensory deficit. Usually complete return of neural function does not occur, distinguishing this from a second-degree injury (Jobe et al., 2016).

In fourth-degree injury, the entire fascicle and its surrounding perineurium is disrupted and is very disorganized. All bundles are breached. The epineurium is intact and continuity of the nerve trunk is maintained, but one cannot delineate the fasciculi from the epineurium.

Neuromas form. The incidence of retrograde degeneration and axonal loss is higher. Wallerian degeneration occurs in the distal stump. During regeneration, axons enter the interfascicular spaces. Some terminate blindly. Very few reach their original distal endoneurial tubes, resulting in spontaneous recovery. Others enter functionally unrelated foreign tubes, thereby changing the pattern of reinnervation (cross-shunting) and resulting in poor and incomplete recovery. If all fascicles are involved, there is complete loss of motor, sensory, and sympathetic function in the distribution of the nerve (Sonabend et al., 2012). Prognosis for significant return of useful function is uniformly poor without surgery (Jobe et al., 2016).

In fifth-degree injury, the nerve is completely transected, resulting in a variable distance between the neural stumps. These injuries occur only in open wounds and usually are identified at the time of early surgical exploration. The likelihood of any significant spontaneous bridging by axonal sprouts is remote, and the possibility of any significant return of function without appropriate surgery is equally remote (Jobe et al., 2016).

Partial and mixed injuries (combined): Sunderland's classification system can be used to describe partial and mixed injuries. In partial lesions, only a portion of the nerve fibers may be injured while the remaining are intact. In mixed (combined) injuries, all parts of the nerve are affected, with some areas more severely affected than others. For example, partial severance or subtotal fourth-degree involvement of the fascicles can coexist with minor degrees of injury to the remaining fibers of the nerve. Fascicles in continuity can contain fibers with neurapraxic, axonometric, or both types of injuries inside the same bundle. There may be complete loss of motor, sensory, and autonomic function in the distribution of the affected nerve(s). The duration, course, and quality of recovery depend on the severity, number, and type of injury to each individual nerve ber or fascicle (Sonabend et al., 2012). Surgical intervention to correct the fourth-degree and fifth-degree components may sacrifice the function of lesser injured fascicles (Jobe et al., 2016).

However, this classification has somewhat limited clinical utility as most nerve injuries are of mixed grade and there is no diagnostic test to discriminate between Sunderland grades II and IV. Currently these Sunderland grades can only be diagnosed histologically (Grinsell et al., 2014).

4. Peripheral nerve surgery

The primary goal of nerve repair is to allow reinnervation of the target organs by guiding regenerating sensory, motor, and autonomic axons into the environment of the distal nerve with minimal loss of fibres at the suture line (Grinsell et al., 2014).

Several techniques have been established for the surgical repair of nerve injuries: neurolysis, primary and secondary nerve coaptation (end-to-end, end-to-side), nerve grafting (Sinis et al., 2009), nerve transfers (Hebert-Blouin et al., 2017) and muscle neurotization (Cederna et al., 2009).

4.1. Neurolysis

Neurolysis, defined as releasing scar tissue surrounding the injured nerve, is indicated when a neuroma-in-continuity is found. In general, external neurolysis, which is completed during the nerve exposition, is sufficient. In select instances, some advocate limited internal neurolysis, or removal of the scar tissue between the various nerve fascicles (Hebert-Blouin et al., 2017).

4.2. Primary and secondary nerve coaptation

In the case of acute nerve injuries, when no loss of nerve tissue is present, nerve stump reconnection can be done by primary nerve coaptation. This primary nerve suture must strictly be performed without inducing tension. Primary nerve repair is recommended in clean, sharp dissections without associated tissue damage and is only possible in the first few hours after the nerve injury (Sinis et al., 2009). This method allows direct delivery of proximal axons to the

distal stump via a single suture line. It also usually permits fascicular alignment, which increases matching between motor and sensory axons and their targets (Hebert-Blouin et al., 2017). This allows a fast regeneration of the transected axons along the distal nerve stump at a rate that can be roughly estimated at 1 mm per day (though depending on several factors such as age and concomitant diseases) and can reach the periphery in a lapse of time that of course is strictly related to the distance between the lesion point and the end organ. The process of axon regeneration is accompanied by a maturation of the regenerated nerve fibers that consists in the increase of axons diameter. This is accompanied in myelinated fibers by the concomitant increase in myelin thickness that depends on the number of lamellae surrounding the axons. Nevertheless, the histomorphometric data, gathered from animal studies, confirm that normal axon counts are never been achieved, since the histo-architecture changes to the classical picture of degeneration and regeneration (small axons, reduced myelin thickness, increasing axon numbers due to axonal sprouting (Sinis et al., 2009).

However, a direct nerve coaptation without tension is possible even up to a few days after trauma (i.e. 5 – 15 days). In these cases an early secondary coaptation of the stumps is accomplished. This procedure differs from the primary nerve coaptation in the time point. Only the freshly injured and reconstructed nerve should be termed primary nerve repair. A secondary nerve coaptation is recommended for injuries where the timing is late and a tensionless suture is still possible. This is normally the case in nerve injuries which are not explored and reconstructed immediately (Jobe et al., 2016).

When feasible, end-to-end reconnection, in which the proximal and distal stumps of the severed nerve are directly sutured, is the favoured choice. However, if a proximal nerve stump is not available or if there is a long-length nerve defect (Kelly et al., 2007) end-to-side repair can act as an alternative.

End-to-side repair is a type of neurorrhaphy involving the coaptation of the distal end of an injured nerve to the side of a normal nerve acting as the donor. The side of the donor nerve for

suture can be incised through the epineurium or through the perineurium, or it may not be incised at all (L. Chen et al., 2017). Drawbacks of this tecnique are the putative damage inflicted on the donor nerve and the variable quality of the regeneration in the recipient nerve (Kelly et al., 2007).

Since end-to-end primary nerve suture, when performed tensionless, achieves the best results, this treatment is the recommended surgical procedure for the injured nerve.

Several techniques for nerve repair have been proposed: epineurial, perineurial, fascicular suture and the adhesive coaptation.

4.2.1. Epineurial nerve suture

The epineurial repair represents the most commonly used technique for nerve repair, and it is still considered the gold standard treatment in case of complete nerve lesion without loss of substance in a well-vascularised bed (Grinsell et al., 2014). Nerve continuity is obtained by connection of the epineurium from the proximal and distal stumps (Figure 5).

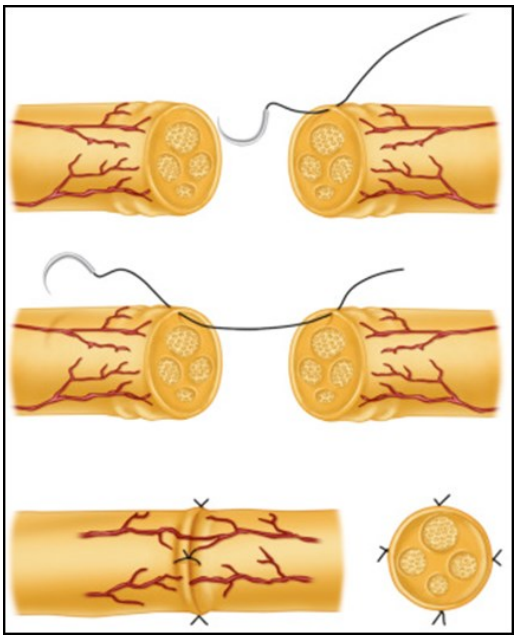

Figure 5. Epineurial nerve suture (Jobe et al., 2016)

A sine qua non for successful nerve regeneration is to perform débridement of both ends of the nerve and resect scar tissue until endoneurium bulges out of the cut sections (L. Chen et al., 2017). In comparison with other techniques it is less traumatic since only the outer connective tissue is used for suture. However, the intraneural contents are not involved in this procedure and fascicular alignment is achieved by placing the sutures among the nerve stumps at the epineurium. The used suture material should always be a 10 -0 microsuture or less and should be applied sparingly since it represents a foreign-body that could prevent regenerating axons from sprouting (Sinis et al., 2009).

4.2.2. Perineurial suture

While in epineurial suture only the superficial connective tissue is stitched, in perineurial suture the perineurium surrounding the internal neural structures is used. The advantage of this technique is that it allows a more precise grouping of the different fascicle groups since the tissue that is stitched lies among the different groups (interfascicular). The drawback, however, is that the suture material lies within the nerve posing the risk of developing a regenerative block due to foreign-body formation (Sinis et al., 2009) (Figure 6).

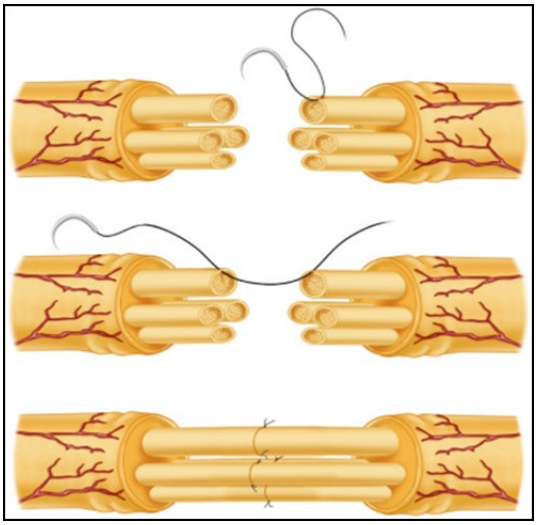

Figure 6. Perineural nerve suture (Jobe et al., 2016).

4.2.3. Fascicular suture

In addition to the perineurial suture techniques the fascicular suture allows the different fascicular groups to be connected directly. This fascicular stitching technique should be applied only epifascicularly using very small suture material (11-0, 12-0) due to a potential damage of the fibers running in fascicular groups. This procedure is recommended in nerve grafting since the donor nerve is smaller compared to the recipient in most cases. Therefore, the transplantation of more than one graft into the defect is necessary. The theoretical advantages of better fascicle alignment with this technique are offset by more trauma and scarring to the healing nerve internally due to the presence of permanent sutures. Despite its anatomical attractiveness, overall group fascicular repair is no better than epineural repair in functional outcomes (Grinsell et al., 2014). The main disadvantages of the fascicular nerve repair, however, is the increasing operative time period and the higher risk for fibrosis at the coaptation sites since the amount of suture material is increased as well (Sinis et al., 2009). For this reason, coaptation of more than five fascicles is not recommended (L. Chen et al., 2017).

4.2.4. Adhesive coaptation

Using the technique of adhesive coaptation, the nerve stumps are connected without suture. Proximal and distal stumps are attached using various substances such as polyurethane, silicone films, fibrin glues, etc. Analysis of the clinical outcome after using different adhesive procedures for nerve repair demonstrated poor results due to the histotoxicity of the materials used and the excessive fibrosis incurred at the suture sites. In contrast, substances such as fibrin glue and factor XIII showed results comparable to conventional suture techniques in animal studies. However, the adhesive coaptation is used only in few centers and the epineurial suture technique remains the gold standard for nerve repair (Sinis et al., 2009).

4.3. Nerve grafting

Direct nerve repair, using either primary or secondary nerve suture techniques, is not always possible. After a nerve injury with tissue loss, a nerve gap may result making it impossible to suture the nerve stumps without tension. Millesi demonstrated that clinical results after the performance of a nerve graft are superior to that of a primary nerve suture performed under tension. The knowledge of this fact became revolutionary since the regenerating axons have to pass two suture sites. There is a 50% loss of axons at each coaptation site. Therefore, for primary nerve repair without tension, approximately 50% of the original axons will successfully regenerate through the repair site. For a nerve graft with two coaptation sites, 25% of axons will successfully regenerate through the graft (Grinsell et al., 2014). Still, further experimental studies demonstrated that regenerating axons pass readily through a nerve graft, with two tension free suture sites, compared to a single suture line under tension (Millesi, 1982, 2000; Sinis et al., 2009). Thus, for longer nerve defects on which direct repair cannot be carried out without excessive tension, nerve grafting is the "gold standard" of repair (L. Chen et al., 2017).

4.3.1. Autologous grafts

The most widespread nerve repair strategy to bridge nerve gaps is the use of nerve autografts, harvested from the patient's own body but from another location ([a]Arslantunali et al., 2014). Autografts are immunologically acceptable and provide the perfect structural and fascicular composition needed for the alignment of the regenerating nerve fibers.

After harvesting the nerve, the autografts are implanted into the nerve defect reversed in orientation to maximize the number of axons successfully regenerating by funneling them distally, thus preventing the loss of regenerating axons down side branches of the graft. The surgeon should try to carefully match the different fascicular groups of the proximal and distal stumps (Sinis et al., 2009) and to pay very close attention to perform a tensionless coaptation.

To this end, and also considering the movement range of the extremity and the retraction and shrinkage of the autograft, the length of the graft should exceed 20-30% of the gap to be bridged. Moreover, since the the nerve stumps are not always composed of regular nerve structures but still filled with scar tissue, it is mandatory to cut them till a clean and healthy section is reached. In difficult cases, histological analysis of intraoperative frozen sections can be used to characterize structures of interest (Jobe et al., 2016).

The harvested autologous nerve graft undergoes Wallerian degeneration (Grinsell et al., 2014). Axonal regeneration is then guided on the surface, mainly consisting of laminin and collagen, of the degenerated graft. This procedure is highly complex and depends on the migration from proximal and distal nerve stumps of one key cell, namely the Schwann cell, that invade the degenerated surface structures on the grafted material (Sinis et al., 2009). These cells also direct the production of several nerve growth factors, i.e. brain-derived neurotrophic factor, glial-derived neurotrophic factor, nerve growth factor, etc, that stimulate the axonal outgrowth and provide trophic support to the regenerating axons (Sinis et al., 2009). Therefore, autologous nerve grafts fulfill the criteria for an ideal nerve conduit because they provide a permissive and stimulating scaffold including Schwann cell basal laminae, neurotrophic factors, and adhesion molecules (Grinsell et al., 2014).

Nerve grafts can be single, cable, trunk, interfascicular, or vascularized. A single graft is a segment of donor nerve of a similar diameter to the nerve to be repaired, while to span gaps between large diameter nerves, multiple lengths of a smaller diameter donor nerve are bundled in a cable grafts (Figure 7) to approximate the diameter of the injured nerve.

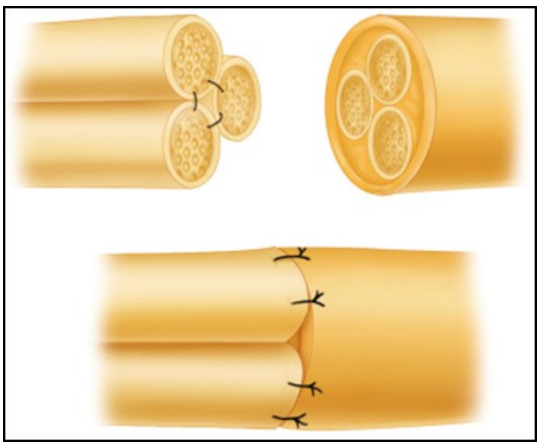

Figure 7. Cable graft (Jobe, 2017).

Trunk grafts use a segment from a large nerve to repair a gap in a proximal nerve. There has been poor success with this method as large diameter donor nerves fibrose internally due to poor vascularity before axons are able to regenerate across the graft (Grinsell et al., 2014). In the interfascicular nerve graft (Figure 8) individual nerve grafts are used to bridge the matching fascicles or fascicle groups at the proximal and distal stumps; the epineurium of the graft is sutured to the interfascicular epineurium or perineurium of the fascicular group (L. Chen et al., 2017).

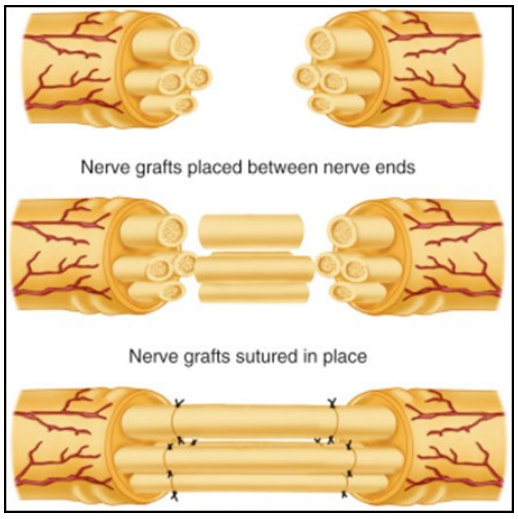

Figure 8. Interfascicular nerve graft (Jobe et al., 2016).

Lastly, in the vascularised nerve graft the donor nerve is transposed with its arterial and venous supply into the graft site. Vascularisation allows a nerve graft to avoid the initial period of ischaemia and ensures continuous nutrition of the graft. Intraneural fibrosis is avoided and axonal regeneration and target connectivity is enhanced (Grinsell et al., 2014). There is no evidence that indicates this is superior to nonvascularized nerve grafts, but vascularized repair makes intuitive sense if the bed of the graft has compromised vascularity (e.g. irradiation or scarred recipient bed) (Kwei et al., 2009).

Despite nerve autografts success rate and prevalence, there are same serious drawbacks to be highlighted. First and foremost, the necessity to sacrifice a donor nerve such compromising the functionality at the donor site. As harvesting nerve grafts should not cause significant motor deficits, sensory nerves are usually chosen as donor sites (Sinis et al., 2009). Functionally less important nerves like sural nerves, superficial cutaneous nerve, or lateral and medial antebrachii cutaneous nerves are the most used. Second, the availability and the length of nerve that can be harvested are limited such that the reconstruction of very long and complex nerve defects may be incomplete. Use of autografts is currently restricted to critical nerve gaps of nearly 5 cm ([a]Arslantunali et al., 2014). Third, causing a second surgery site which is associated with donor site morbidity (i.e. infection or neuroma formation) and increased operative and recovery time. Fourth, possible mismatch in axonal size, distribution, and alignment that limits the regeneration capacity of the autografts (Jobe et al., 2016). Fifth, the time lapse between trauma and operation, the length of the gap, the distance to the motor/sensory target, the age of the patient, and the type of injury can have a strong negative influence on the outcome.

Due to the described drawbacks and limitations, the variability of clinical results, and the potential side-effects of autologous nerve grafting, the research of alternative grafting materials has been a major endeavor for surgeons engaged in peripheral nerve surgery (Sinis et al., 2009).

4.3.2. Allografts

Nerve allograft is a technique used to bridge a peripheral nerve lesion with tissues derived from a different individual of the same species. An allograft nerve tissue serves as a support for guidance and a source for viable donor-derived Schwann cells that would facilitate the connection of axons at the proximal and distal ends to achieve reinnervation of target tissue or organs (Sinis et al., 2009). Compared to autografts the use of allografts has no donor site morbidity, is less time consuming in surgery, may provide better nerve samples (in terms both of quantity and caliber), and it requires no surgical adaptation of the diameter stump between donor and recipient nerves (Squintani et al., 2013). On the contrary, there are significant costs and complexity with their use. In particular, the use of allografts presents limitations including immune rejection, risk of cross contamination, and secondary infection. Therefore, the use of allografts requires systemic immunosuppressive therapy (for up to two years, until the donor nerve graft has been repopulated with host Schwann cells (Grinsell et al., 2014), which is not a desirable treatment due to increased risk of infection, decrease of healing rate, and secondary neoplasm formation and other systemic effects ([a]Arslantunali et al., 2014). Considered this, nerve allotransplantation should be reserved for unique patients with irreparable peripheral nerve injuries, which if left untreated, would lead to an essentially nonfunctional limb (Sinis et al., 2009).

Currently, there are protocols which encourage the use of decellularized nerves to reduce the immunogenicity of nerve allografts while preserving the extracellular matrix. However, currently their use like hollow conduits is limited to small sensory nerves, for example, digital nerves, for gaps less than 3 cm. Moreover, decellularized nerve grafts are not considered a replacement for autologous nerve grafting in motor nerves, gaps more than 3 cm, or in proximal nerve injuries (Sinis et al., 2009).

4.4. Nerve transfers and muscle neurotization

Nerve transfers consist of the transfer of an expandable or redundant working nerve, branch, or fascicle to a nonfunctioning nerve (Hebert-Blouin et al., 2017). Muscle neurotization is a technique that can be used to reinnervate a muscle when there is no distal nerve segment available for end-to-end neurorrhaphy. The proximal end of the severed nerve is surgically placed into the belly of the denervated muscle in the region of the motor endplates (Cederna et al., 2009).

4.5. Tubulization

Although implantation of an autologous nerve graft is accepted as the gold standard therapy for peripheral nerve gap repair, this technique is not always feasible and has inherent drawbacks. Collectively these disadvantages have encouraged the development of alternatives to autologous nerve grafts (Gu et al., 2014).

In general, the alternative graft should: a) provide a channel to the sprouting axons, such that they can reach the distal stump and reinnervate the end organ (Sinis et al., 2009); b) maintain adequate mechanical support for the regenerating nerve fibers; c) provide a conduit channel for the diffusion of neurotropic and neurotrophic factors secreted by the damaged nerve stump and a conduit wall for the exchange of nutrients and waste products; d) obviate the infiltration of fibrous scar tissue that hinders axonal regeneration; e) create an optimal microenvironment (niche) for nerve regeneration through the accumulation and release of exogenous and endogenous biochemical effects (Gu et al., 2011) (Figure 9); moreover, it has to be easy to manufacture and sterilize, and inexpensive.

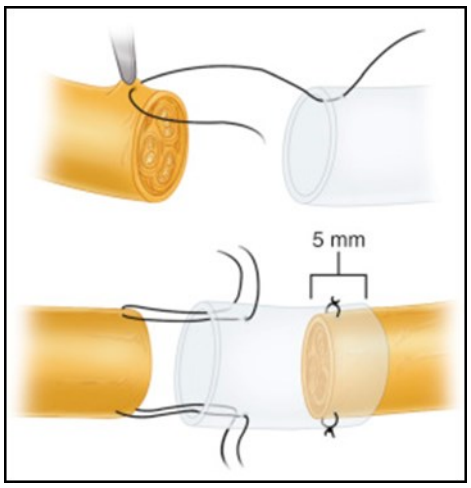

Figure 9. Interposition of a neural scaffold (Jobe, 2017).

Transparency is preferred for suturing and accurate positioning of the nerve stumps (de Ruiter et al., 2009).

From a histopathological point of view, once implanted, the conduit promotes the regenerating axons facilitating the migration of Schwann cells and the accumulation of neurotropic factors. Inside the conduits, the wound healing response results in the formation of a fibrin matrix in the lumen and across short lengths. This fibrin matrix accommodates Schwann cells, fibroblasts, and macrophages (Pabari et al., 2014).

Autologous non-nerve tissues (i.e. bone, artery, vein, or muscle) have been widely used for this purpose; however, they are not devoid of disadvantages. Low outcomes, lack of suitable donor vessels, venous lumen collapse, growth of nerve fibers out of the muscle tissue during regeneration, and the necessity of a donor site have led surgeons and researchers to turn their attention towards different grafts made of biological or artificial polymers (Gaudin et al., 2016).

4.5.1. Properties of synthetic neural scaffolds

Any biomaterial used to prepare neural scaffolds (both of natural or synthetic origin) should possess appropriate physicochemical, biomechanical and biological properties. Here are summarized the most relevants:

a) Mechanical strength and flexibility

These tensile properties are important because a nerve tube should be flexible for implantation but at the same time, the nerve tube should be resistant to deformation (elongation, breaking, or kinking) and strong enough to hold a suture (de Ruiter et al., 2009). Therefore, it is mandatory to make the right balance between the flexibility and hardness, as too stiff scaffolds are easy to cause dislocation, and too flexible scaffolds fail to support axonal regeneration (Gu et al., 2011). It is important to note these physical properties of the nerve tube depend not only on the biomaterial but also on other factors, such as the dimensions of the nerve tube, the thikness, the lumen diameter and fabrication technique (de Ruiter et al., 2009).

b) Porosity and permeability

A neural scaffold must have a sufficient permeability for nutrient and gas exchange (Shi et al., 2009), including the exchange of fluids between the regeneration environment and surrounding tissues, avoiding the buildup of pressure due to fluid retention (Gu et al., 2011).

A solid or nonporous conduit would prevent the diffusion of nutrients into the lumen while retaining undesirable waste products. The overall implication is that there is a restriction in nerve growth. A highly porous conduit, on the other hand, would allow trophic factors to diffuse out from the conduit. This loss would prevent axons from attaining their optimal growth. An obvious compromise is to use a conduit with an intermediate porosity to allow diffusion of small molecules such as simple nutrients and wastes but provide at least some retention of larger molecules such as growth factors (Rutkowski et al., 2002). A maximum in the growth of axons occurs at a porosity of 75%. A higher porosity likely leads to a loss of neurotrophic factors from the lumen, thus decreasing growth. Moreover increased porosity leads to enhanced oxygenation (the minimum requirement for nerve growth in vivo is 2 μg/mL) (Rutkowski et al., 2002). Permeability however not only depends on pore size but may also be affected by, for example, hydrophilic properties of the material (de Ruiter et al., 2009).

c) Surface properties

Surface properties, including surface functionalization, are a dominating factor in affecting the interactions between a neural scaffold and nerve cells (Gu et al., 2011). With smooth surfaces (eg, in silicone nerve tubes), the longitudinal matrix coalesces and forms a free-floating nerve cable, whereas with rough surfaces, the tissue disperses and completely fills the lumen of the nerve tube (de Ruiter et al., 2009). Instead, a longitudinally oriented surface texture of the neural scaffold has been shown to influence directional outgrowth of axons and uniform alignment of Schwann cells in vitro, and to result in an improved nerve regeneration in vivo (Gu et al., 2014).

d) Biocompatibility

Refers to an ability to serve as a substrate that supports the appropriate cellular behaviors, including the promotion of molecular and mechanical signaling systems to aid nerve regeneration, without eliciting any undesirable effects on neural cells and tissues and/or inducing any undesirable local or systemic responses in the eventual host. The biocompatibility of neural scaffolds can be evaluated from three aspects of blood compatibility, histocompatibility, and mechanical compatibility. Blood compatibility requires that the scaffold in contact with blood does not induce hemolysis, destroy blood components, or lead to coagulation and thrombus formation. Histocompatibility means that the scaffold has no toxic side effects on the surrounding tissues, while the surrounding tissues, in turn, do not induce corrosive effects or immune rejection on the scaffold (Gu et al., 2011).

Although many biomaterials are essentially non-toxic, non-allergic, non-mutagenic and non-carcinogenic, they are likely to trigger a wide variety of unwanted responses in the human body (Malik et al., 2011). Moreover, the ideal biomaterial should not behave as a inert structure, but should be able to positively influence the performance of the target cell, otherwise functional recovery will be significantly compromised (Gu et al., 2011).

e) Biodegradability

An ideal scaffold has to possess a controllable ability to degrade in vivo, undergoing a process a process of resorption after successful regeneration, without eliciting toxic metabolites (Sinis et al., 2009). The ideal neural scaffold should remain intact for the time axons need to regenerate across the nerve gap and then degrade gradually with minimal swelling and foreign body reaction (de Ruiter et al., 2009).

4.5.2. Biomaterials for nerve conduits

To meet the requirements described above, the researchers have tried to improve the outcomes of grafting turning their attention towards many different materials (Siemionow et al., 2010) which can be grouped into two distinct generations that have clinical relevance and a third one that is still under development.

a) The First Generation

The initial strategy to develop a synthetic conduit was to design a support structure that would guide regrowth of the transected nerve and provide a stable barrier against the infiltration of connective tissue. The first artificial conduit generation was tubes of nonresorbable silicone or polytetrafluoroethylene (ePTFE, Gore-Tex) (Gaudin et al., 2016).

Due to the inert and elastic properties of silicone rubber, silicone tubes represent one of the first and most frequently used neural conduits, they are nondegradable in the body and impermeable to large molecules (Gu et al., 2011) and they only supply an isolated environment for nerve regeneration (S. Wang et al., 2010). Although in some cases satisfactory regeneration was reported, compression syndromes or fibrotic encapsulation of the implant occurred following successful regeneration. The tubes had therefore to be removed in a second surgical intervention (Gaudin et al., 2016). For these reasons, in periods of new innovation in basic material science,

silicone implantation for reconstruction of peripheral nerves is no longer of interest (Sinis et al., 2009).

Polytetrafluoroethylene (PTFE) is a highly inert material due to its chemical structure consisting of fluorine and carbon atoms. The first reports of PTFE tubulization demonstrated excellent motor and sensory recovery in humans. Further studies, however, could not reproduce these results since regeneration was histologically evident while the recovery of function was poor. Due to the knowledge gathered from the application of silicone tubes the PTFE tubes were never widely clinically applied (Sinis et al., 2009).

Due to the important drawbacks of nonresorbable conduits, new approaches in material sciences have been therefore directed towards resorbable materials, called "biocompatible" materials (Sinis et al., 2009).

b) The Second Generation

Second-generation nerve conduits are constructed from resorbable material, are biocompatible, and have specific tube wall structures. These conduits aim to increase functional rehabilitation and axonal remyelination through enhancement of material biocompatibility and topography (Gaudin et al., 2016).

Provided that such materials degrade with minimal tissue reaction and without impairment of nerve regeneration (de Ruiter et al., 2009), it is imperative that their degradation time is comparable to the time taken for the nerve to heal. Too rapid degradation rate may result in failing to protect regenerated axons, and too slow degradation rate may lead to compression and foreign body reaction (Gu et al., 2014). Although immune reactions may also be initiated by biodegradable materials, conduits can be engineered to be nontoxic or result in delayed toxicity, such that most of the material is degraded before initiating an immunologic response (Pabari et al., 2014). To find a material that fulfil all these requirement is not an easy task but, although the perfect one is yet to be found, many are widespread in clinical use.

Type I Collagen. Collagen is the most commonly used material for conduit fabrication. It is an important structural protein that is found ubiquitously in the body, for example, as fibrils in the endoneurium or as a non-fibrillar component in the basal lamina (Gaudin et al., 2016). Type I is the most common collagen and is the principal collagen type in skin and bones and is also the predominant collagen in the intact peripheral nerve. Collagen types I and III together constitute 49% of total protein in nerves (Meek et al., 2008). Being one major form of extracellular matrix (ECM) protein, collagen provides excellent biocompatibility and weak antigenic activity, supporting tissue healing and cellular proliferation (Gaudin et al., 2016). Both collagen type I and type III can be derived from animal tissues such as porcine skin and bovine deep flexor (Achilles) tendon (S. Wang et al., 2010). However, collagen type I is often used as a medical implant versus other types of collagen because it is more abundant and can be isolated and purified by well-established conventional techniques (Meek et al., 2008). Once purified, collagen hydrogels are then easily generated from fibrillar collagen sheets, which are rolled into three-dimensional nerve conduits (Gaudin et al., 2016). Type I collagen-based implants have been proven to support and guide tissue regeneration in vivo (Meek et al., 2008) and has been demonstrated capable of splinting small nerve defects up to 20mm (Gaudin et al., 2016). As the degradation rate of collagen tubes has been reported to occur between 1 and 9 months, depending on the different fabrication methods used (Meek et al., 2008), it is raises the concern that degradation may occur before nerve regeneration process is completed depending on the size of the nerve defect. Currently however, there are several collagen-based nerve conduits that have been U.S. Food and Drug Administration (FDA)– approved and are commercially available.

Polyglycolic Acid. The polyglycolic acid (PGA) material is a porous mesh, which allows the infiltration of oxygen to support the regeneration process. The PGA tube is flexible to accommodate movement of joints and associated tendon gliding. It is corrugated to resist occlusive force of surrounding soft tissue. The material is already widely used in absorbable

Vicryl sutures and sheaths for many different applications (Meek et al., 2008) and its conduits are already FDA– approved and commercially available for peripheral nerve regeneration (Pabari et al., 2014).

The degradation time is approximately six to twelve months. However, there is a concern that PGA conduits might degrade before the nerve regeneration process is completed and that its lactic acid degradation product may have toxic effects. Extrusion of PGA conduits has also been reported (Gaudin et al., 2016).

Caprolactone Conduits. A poly-D,L-lactide-co-epsilon-caprolactone conduit (P(LL-co-CL)) consists of lactic acid and caprolactone monomers. Caprolactone nerve tubes are normally stiff and only flexible after putting in warm saline before implantation (de Ruiter et al., 2009). The consequence may be frequent breaking of the needle when using a small needle. Introducing bigger needles and sutures introduces more damage and foreign body reaction. The stiffness of caprolactone nerve conduit may lead to inflexibility over joints during mobilization. In turn, the nerve stump may be torn out of the lumen of the tube (Meek et al., 2008). According to literature also, these transparent conduits may produce fewer toxic degradation side products and have a long degradation time up to 16 months (Gaudin et al., 2016). This longer degradation time may also be disadvantageous, as it is possible that this results in granuloma formation in the longer term. There is currently one FDA approved synthetic caprolactone conduit on the market (Meek et al., 2008). Although the caprolactone nerve guide has been shown to be as effective as autologous nerve grafts for small nerve gaps, it once again does not surpass the criterion standard method (Pabari et al., 2014).

Polyvinyl Alcohol (PVA). Polyvinyl alcohol (PVA) is a non-toxic synthetic polymer approved by the FDA for biomedical and biotechnological applications. PVA can form gels in acqeous solution at room temperature or through the cryogelation technique. Cryo-PVA gels find various applications in biomedicine due to their biocompatibility, elasticity, permeability both to oxygen and to low molecular weight molecules such as nutrients and drugs. Despite PVA is

a nondegradable material, its elasticity prevents compression syndromes. PVA does not support cell growth and proteins adhesion, however, the material can be partially modified by oxidative methods, in order to increase both the degradation rate and the potential molecular binding sites. Currently, PVA conduits have been approved by the FDA as the only nondegradable synthetic nerve guide (Gaudin et al., 2016). So far, few papers are present in literature describing the use of PVA as a biomaterial for the regeneration of peripheric nerves and no information about the repair effcacy of these conduits has been reported in peer-reviewed journals (Gaudin et al., 2016).

Fibroin. Silks are fibrous polymers of animal head-spring. Silk obtained from cocoons of mulberry silkworms (i.e. Bombix mori) is popularly known in textile industry as dress tissues and has been used for centuries in medicine as a wound dressing and as suture fibers due to its strength and bio-compatibility. Silk worms can be raised in captivity on large scale for textile manufacturing, therefore this natural polymer is abundant and inexpensive. The raw cocoon filament consists of two main proteins, sericin and fibroin, fibroin being the fiber core of the silk, and sericin being the sticky material surrounding it. For medical applications adequate extraction of sericin is required because of its irritant effect. In addition, the surface of the degummed fibroin silk can be chemically modified to change its properties such as degradation rate or to link growth factors. Fibroin has been rigorously studied with superior biocompatibility and low immunogenicity, and it is slow-rate degradable with excellent mechanical stability and high resilience (S. Wang et al., 2010). For nerve repair it can easily be integrated in a tubular-like structure (Gaudin et al., 2016). Several recent studies demonstrated a good potential for fibroin in reconstruction of peripheral nerves in vitro and in vivo (Huang et al., 2012; Park et al., 2015). Despite the very promising results of fibroin conduits neither the FDA nor any other administration has yet approved any silk conduit (Gaudin et al., 2016).

For smaller (< 3 cm) nerve defects, second-generation nerve conduits provide sufficient guidance for regeneration, yielding as good results as autologous nerve grafts with the practical

advantage of an unlimited right-off-the-shelf availability in different sizes and without the severe dawbacks (de Ruiter et al., 2009). Moreover, the in vivo interactions between scaffolds and host cells/tissues are complex and bi-directional: not only will the scaffold elicit cell and tissue responses, but host cells/tissues will change the local environment provided by the scaffold through deposition of ECM molecules (Pancrazio et al., 2007). However, a satisfactory outcome in bridging larger nerve defects still remains a challenge (Gaudin et al., 2016) and identifying a suitable biomaterial is the key to meet it.

c) The Third Generation

The third generation of conduits, which is not FDA approved and still in early steps of research, is more of composite types in order to maximize biological–mechanical–chemical response (Goonoo et al., 2016) through a systematic combination of molecular and mechanical signals.

The aim of this tissue-engineered scaffold is to exploit those strategies that can actively delivery cues to cells, taking part in replicating, as far as possible, the niche of target cells (Gu et al., 2014).

Different modifications to the common hollow or single lumen nerve tube have been investigated to enhance regeneration and extend the gap that can be bridged (de Ruiter et al., 2009), such as controlled release/delivery of neurotrophic factors, electroconductive material, stem or Schwann cells, extracellular matrix proteins, surface micropatterning, or luminal fillers as guidance structures with favorable physical and mechanical properties (Gaudin et al., 2016).

4.6. Surgical timing

The controversy regarding the timing of nerve repairs in general is unresolved (Jobe, 2017). Delay of neurorrhaphy affects motor recovery more profoundly than sensory recovery, most likely because of the survival time of denervated striated muscle. For every delay of 6 days between injury and repair there is a variable loss of potential recovery that averages about 1%

of maximal performance; after 3 months, this loss increases rapidly. The influence of delay on sensory return is unclear (Jobe et al., 2016). Generally, however, the longer the delay in repair, the poorer the return of motor function that can be expected. The reinnervation of denervated muscle may occur 12 months later; however, after that period, irreversible changes occur in the muscle cells and there is little hope of recovery of motor function after reinnervation. The return of sensation has been observed when nerve repair has been performed 2 years after injury. Delay in nerve repair assumes the following: (1) muscle atrophy occurs, (2) contraction in the endoneural tubules of the distal segment progresses, (3) retraction of the nerve ends may occur, (4) joint contractures may develop, (5) a second operation is involved, and (6) intraneural alignment of fascicles may be more difficult. Additional factors to consider in the timing of peripheral nerve repairs include the condition of the patient and the state of preparedness of the surgeon and the institution, including the availability of instruments and personnel to allow a satisfactory primary repair (Jobe, 2017). Late surgery, occurring more than 1 year after injury, may be considered a salvage procedure in patients who are seen in a delayed fashion or in those who either have not recovered or have recovered incompletely after spontaneous recovery or previous nerve surgery. However, reconstructive options addressing muscles, tendons, bones, and joints may be useful (Hebert-Blouin et al., 2017).

5. Animal model for research on nerve conduits

Research into the use of nerve conduits has been performed predominantly in mice, however also rabbits and monkeys have been used, being the primate model the closer-to-human comparison model but the most infrequent (de Ruiter et al., 2009).

Although convenient, rodents demonstrate superior neuroregenerative capacity compared with higher mammals and humans. In rodents, late–time point observations may show positive and negative groups to be equivalent because of the superior regenerative capacity of the rodent nervous system masking differences between these groups. In addition, the diameters of even

the largest nerves used in animal models are smaller than human nerves, such that human physiologic conditions are difficult to be mimicked in animal models. Therefore, when extrapolating the results of animal studies to humans, the diameter of the animal nerve and the relative diameter of nerve and conduit should be considered carefully, as both will affect the concentration of the neurotrophic factors necessary for nerve regeneration (Pabari et al., 2014). In rodent's animal model, the sciatic nerve is the most common choice, as it is the biggest nerve available. The sciatic nerve is a mixed nerve, composed of fibers from L4, L5, S1, S2, and S3. With its motor component, it supplies the muscles of the entire leg and foot and the posterior part of the thigh, and then carries most of the sensory fibers from these same parts.

AIM OF THE STUDY

The management of peripheral nerve injuries is a challenge to both patient and surgeon especially in case of neurotmesis with loss of substance. A satisfactory outcome in bridging larger nerve defects remains a challenge; hence, identifying a nerve conduit with these capabilities remains an ambitious goal.

Considered this, the aim of the present study was to investigate *in vitro* and *in vivo* (animal model: Sprague-Dawley rat) the characteristics and the regenerative potential of three different nerve conduits made up of PVA; 1% Oxidized PVA (1% Ox PVA) and Silk-Fibroin.

PVA conduits have been approved by the United States FDA as the only non-degradable synthetic nerve guide (SaluBridge; SaluTunnel; SaluMedica LLC, Atlanta,GA, USA). So far, no information about the repair efficacy of these conduits has been reported in peer-reviewed journals. 1% Ox PVA is a novel biomaterial we patented; in comparison to the native form, it possesses a certain biodegradation rate which should be adequate to sustain nerve regeneration. Silk-Fibroin is a natural polymer demonstrating a good potential in reconstruction of peripheral nerves *in vitro* and *in vivo*. Despite the very promising results of Silk-Fibroin conduits, neither the FDA nor any other administration has approved any silk conduit.

The experimental study was structured as follows:

1) Preparation of polymer solutions (PVA, 1% Oxidized PVA and Silk-Fibroin solutions).

2) Manufacture of PVA, 1% Oxidized PVA and Silk-Fibroin disk-shaped supports.

3) *In vitro* studies.

- Morphological characterization of disk-shaped supports by Scanning Electron Microscopy.
- Evaluation of the biocompatibility/biologic activity of the biomaterials by Scanning Electron Microscopy and MTT assay. A Schwann cell line (SH-SY5Y) was used for this purpose.

4) Manufacture of PVA, 1% Oxidized PVA and Silk-Fibroin tubular scaffolds.

5) *In vivo* studies.

- Grafting of PVA, 1% Oxidized PVA and Silk-Fibroin tubular scaffolds in animal models (Sprague-Dawley rats) of peripheral nerve injury with loss of substance (nerve gap: 5 mm).
- Evaluation of the functional recovery of animals at 12 weeks after surgery.
- Euthanization of animals at 12 weeks after surgery and *in situ*-evaluation of the implanted samples.

6) Explantation of the grafts and analysis of the specimens.

- Histological (haematoxylin and eosin staining) and immunohistochemical (anti-CD3; anti-S100 staining) analysis.
- Evaluation of the axonal regeneration by Toluidine Blue staining and Transmission Electron Microscopy.
- Histomorphometric analysis.

MATERIALS AND METHODS

1. Polymer solutions

Three different polymer solutions (PVA, 1% Ox PVA and SF) were prepared. Thereafter, these will be useful in the preparation of the supports.

1.1 Preparation of PVA polymer solution

PVA solution was obtained by suspending in MilliQ water a certain quantity of PVA powder (molecular weight [Mw] 146 000–186 000 Da, 99+% hydrolyzed; Sigma-Aldrich Chemical Company, St. Louis, MO, USA) and heating the suspension until the polymer was completely dissolved (48 h at 100 °C under stirring).

1.2 Preparation of 1% Ox PVA polymer solution

Regarding 1% Ox PVA, partial oxidation of PVA occurred according to a method we patented based on a controlled chemical oxidative reaction (Stocco et al. 2015). Briefly, PVA oxidation was performed in 4 stages described below.

a) PVA dissolution.

A pre-weighted quantity of PVA powder (Molecular weight (Mw) 146,000-186,000 Da, 99+% hydrolysed) was suspended in MilliQ water (16% w/w solution). Powder suspension was than heated for 48 hours (h) at 100 °C, under stirring, until polymer was completely dissolved.

b) Preparation of oxidant solution.

Partial oxidation of PVA was obtained using potassium permanganate ($KMnO_4$) in dilute perchloric acid ($HClO_4$). The required amount of potassium permanganate ($KMnO_4$), was weighed accurately and dissolved in deionized water under stirring. The environment was acidified by addition of perchloric acid ($HClO_4$) at 70%.

c) Oxidation of PVA.

The oxidant mixture was poured rapidly in PVA solution, stirred vigorously, and allowed to react in a thermostatic bath at 30 °C until complete discoloration of the polymer solution. Discoloration occurred in about 60 min.

d) Dialysis against deionized water.

Oxidized solution was poured in a membrane with 8,000 Da cut-off and dialyzed extensively against deionized water under stirring for 48h. Water was replaced every 6 h.

For our purposes, was prepared a PVA solutions with an oxidation degree of 1%.

Typically, to prepare 1% Ox PVA, one gram of PVA was solubilized in 20 ml of MilliQ water and then 5 ml of $KMnO_4$ water solution [2.9 μg/ml] and 0.3 ml of 70% $HClO_4$ were added.

The stoichiometry of the reaction is described by the following equation, referred to a hypothetical vinyl alcohol monomer (- CH_2CHOH -):

$$2KMnO_4 + 5[CH_2CHOH] + 6HClO_4 \rightarrow 5[CH_2CO] + 2Mn(ClO_4)_2 + 8H_2O + 2KClO_4$$

1.3 Preparation of SF polymer solution

Silk Fibroin solution was set up from bombyx mori silk cocoons according to a protocol described by Rockwood et al. (2011) (Figure 10). Briefly, silk cocoons were minced into small pieces and degummed by boiling into an alkaline solution of sodium carbonate (Na_2CO_3 0,02 M) for 30 min. Hence, silk fibroin fibers were rinsed for three times in distilled water to remove the sericin and dried overnight. Thereafter, SF solution was prepared by dissolving 10 g of degummed silk in 9.3 M LiBr solution at 60 °C for 4 h. The fibroin solution was dialyzed in a cellulose membrane based dialysis cassette (molecular cut-off 12,400) against deionized water for 48 h, changing water every 6 h in order to remove LiBr. After dialysis, SF solution was centrifuged twice at 5-10℃ and 9000 rpm for 20 min. The concentrated solutions were stored at 4 °C for further study.

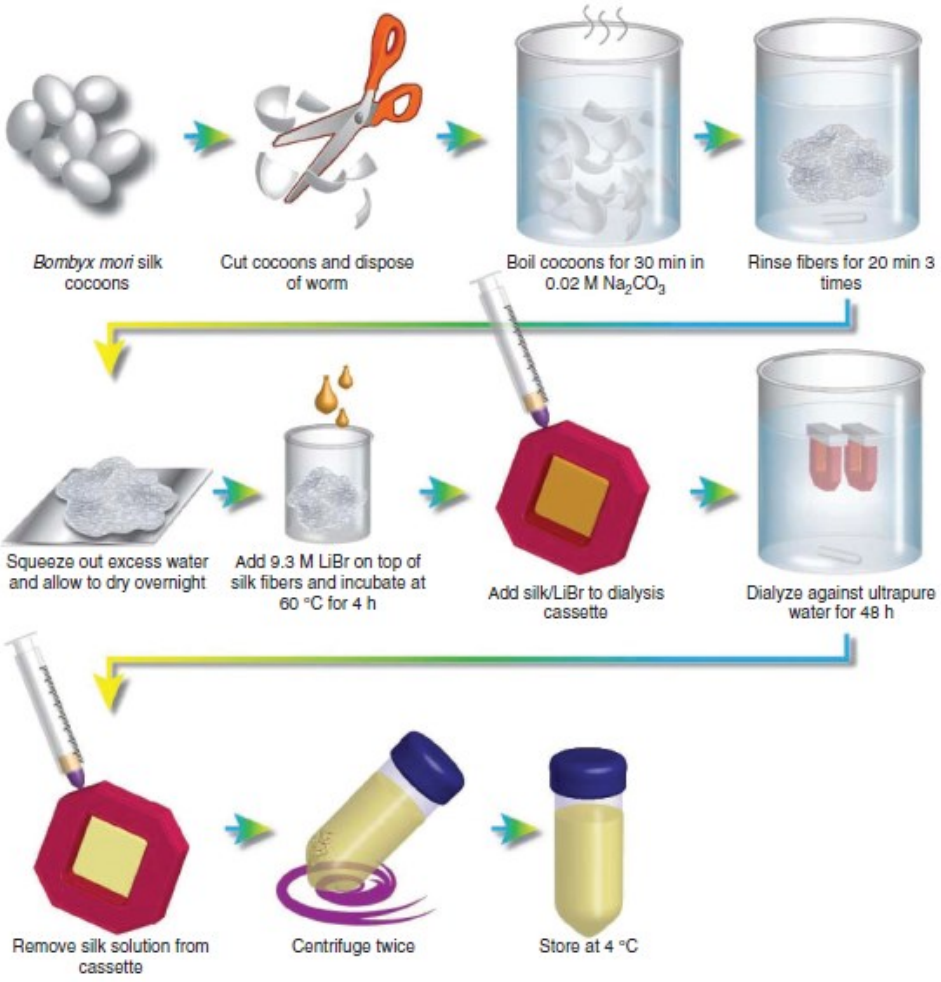

Figure 10. Schematic of the silk fibroin extraction procedure (Rockwood et al., 2011).

2. Manufacture of supports

After preparing polymer solutions, disk-shaped scaffolds and nerve conduits were manufactured; the first will be used for *in vitro* tests; the seconds for *in vivo* implants.

2.1 PVA and 1% Ox PVA disk-shaped scaffolds

Regarding disk-shaped scaffolds, a volume of 0.4 mL of PVA and 1% Ox PVA polymeric solutions respectively were poured in proper molds represented by each well of a 24-well tissue culture plate (BD Falcon, Franklin Lakes, NJ, USA). Hence, a physical cross-linking process occurred; the solutions were first frozen at -20 °C for 24 h and then thawed at -2.5 °C for 24 h. After three freezing-thawing (FT) cycles, the resulting hydrogels were stored at -20 °C until

use.

Aqueous PVA solutions can be chemically crosslinked through the formation of acetal linkages using difunctionally crosslinking agents (i.e., formaldehyde and glutaraldehyde) or by electron beam or gamma irradiation. However, it is well known that these solutions can be transformed into hydrogel even via crystallite formation from repeated freezing thawing cycles, without any chemical crosslinkers that may lead to toxicity. Briefly, during exposure to cold temperatures water freezes, expelling PVA and forming regions of high PVA concentration. As the PVA chains come into close contact with each other, crystallite formation and hydrogen bonding occur. These interactions remain intact following thawing and create a non-degradable three-dimensional hydrogel network (Figure 11). By increasing the number of freeze–thaw cycles and modulating temperature ranges, the degree of polymer phase separation, crystallite formation, and hydrogen bonding can be increased (Holloway et al., 2011; Spiller et al., 2011). Hence, hydrogel mechanical properties can thus be tailored (Kim et al., 2015).

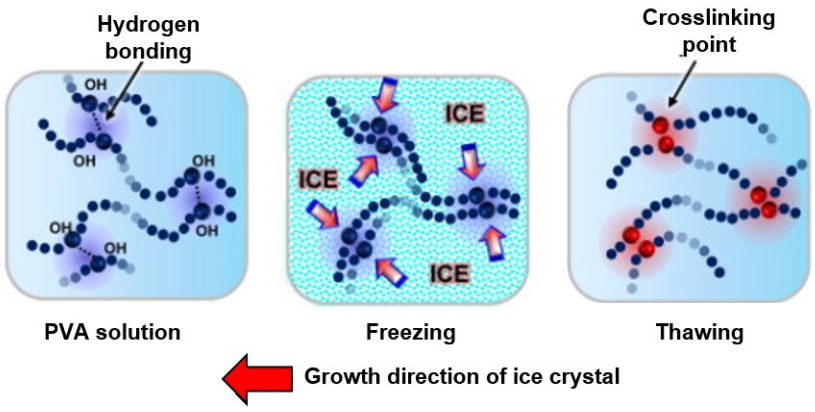

Figure 11. Schematic diagrams showing the mechanisms for (A) hydrogel formation of PVA solution by a freezing–thawing method (Kim et al., 2015).

All prepared PVA-based disk-shaped scaffolds were washed 4 times of 2 h each in PBS solution (0.1 M, pH 7.4) containing 2% penicillin/streptomycin prior to use.

2.2 SF disk-shaped scaffolds

SF disk-shaped scaffolds were manufactured by pouring a certain volume of SF solution (prepared as previously described – see paragraph 1.3) in proper molds represented by each well of a 24-well tissue culture plate. Once poured, the solution was dried over-night and then each scaffold was incubated in 70% Methanol-Water for 2 h. This latter treatment converts the fibroin structure into a beta-structure (Figure 12). Finally, the supports were carefully removed from the molds.

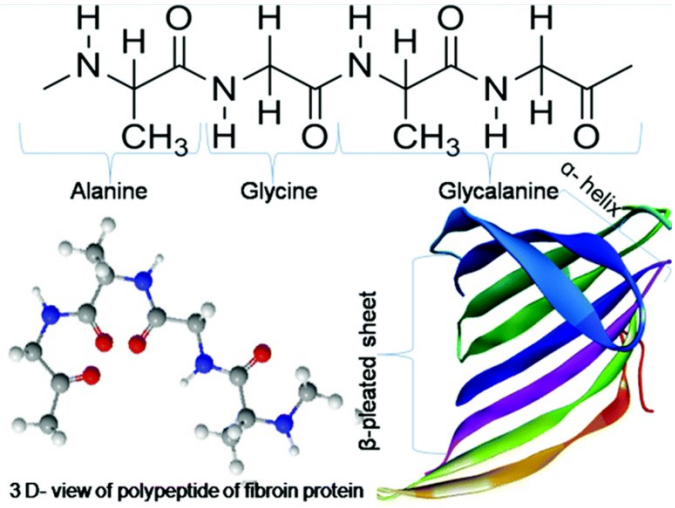

Figure 12. Silk Fibroin beta-structure

All prepared products were disinfected with 70% alcohol and washed with phosphate buffered saline (PBS, 0.1 M, pH 7.4) prior to use.

2.3 PVA and 1% Ox PVA tubular scaffolds

PVA and 1% Ox PVA nerve conduits were manufactured according to the injection molding-technique. Briefly, PVA and 1% Ox PVA polymeric solutions were poured in a proper tubular mold (internal diameter: 2.1 mm) equipped with a central coaxial mandrel (diameter: 1.2 mm) (Figure 13); thereafter, FT occurred as previously described.

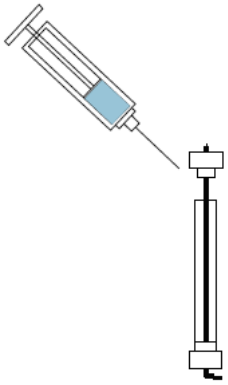

Figure 13. Injection molding technique (Wang et Cai, 2010).

All prepared PVA-based tubular scaffolds were washed 4 times of 2 h each in PBS solution (0.1 M, pH 7.4) containing 2% penicillin/streptomycin prior to use.

2.4 SF tubular scaffolds

SF nerve conduits were manufactured according to the mandrel-coating technique. Briefly, a glass mandrel (diameter: 1.6 mm) was dipped into the SF solution to form a thin polymer layer (Figure 14); after drying for 30 min at room temperature, six coating cycles were performed. Hence, solvent evaporation occurred over-night allowing the formation of the SF scaffold. This step was repeated six times before incubation in 70% methanol-water for 2 hours, this latter treatment converts the fibroin structure into a beta-structure. Finally, the silk cylinder was carefully removed from the mold.

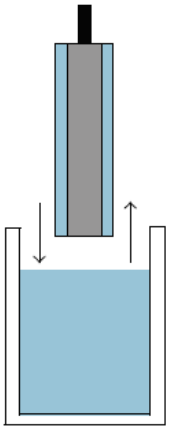

Figure 14. Dip-coating technique (Wang et Cai, 2010).

All prepared products were disinfected with 70% alcohol and washed with phosphate buffered saline (PBS, 0.1 M, pH 7.4) prior to use.

3. Morphological characterization of supports

3.1 *Scanning Electron Microscopy: principles of the technique*

A Scanning Electron Microscope (SEM) provides details surface information by tracing a sample in a raster pattern with an electron beam.

An electron gun generates a beam of energetic electrons down the column and onto a series of electromagnetic lenses. These lenses are tubes, wrapped in coil and referred to as solenoids. The coils are adjusted to focus the incident electron beam onto the sample; these adjustments cause fluctuations in the voltage, increasing/decreasing the speed in which the electrons come in contact with the specimen surface. Using a computer, the SEM operator can modulate the beam to control magnification as well as determine the surface area to be scanned. The beam is focused onto the stage, where a solid sample is placed (Figure 15).

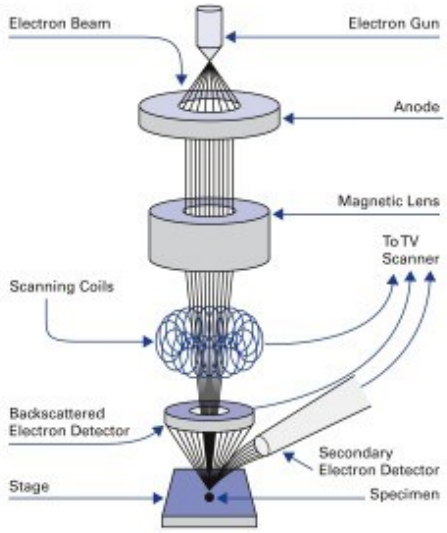

Figure 15. Principal design of a scanning electron microscope (SEM)

Most samples require some preparation before being placed in the vacuum chamber. Among the different preparation processes, the two most commonly used prior to SEM analysis are: a) sputter coating for non-conductive samples; b) dehydration of most biological specimens. In addition, all samples need to be able to handle the low pressure inside the vacuum chamber. The interaction between the incident electrons and the surface of the sample is determined by the acceleration rate of incident electrons, which carry significant amounts of kinetic energy before focused onto the sample. When the incident electrons come in contact with the sample, energetic electrons are released from the surface of the sample. The scatter patterns made by the interaction yields information on size, shape, texture and composition of the sample. A variety of detectors are used to attract different types of scattered electrons, including secondary and backscattered electrons as well as x-rays. Backscatter electrons are incidental electrons reflected backwards; images provide composition data related to element and compound detection. Diffracted backscatter electrons determine crystalline structures as well as the orientation of minerals and micro-fabrics. X-rays, emitted from beneath the sample surface, can provide element and mineral information.

SEM produces black and white, three-dimensional images. Image magnification can be up to 10 nm and, although it is not as powerful as its TEM counterpart, the intense interactions that take place on the surface of the specimen provide a greater depth of view, higher-resolution and, ultimately, a more detailed surface picture.

3.1.1 SEM analysis of disk-shaped supports

The morphological characteristics of disk-shaped supports were investigated by SEM. Samples were dehydrated in graded series of ethanols according to routine protocols; thereafter they were exposed to critical-point drying and gold sputtering and finally observed. Images were taken by JSM-6490 Scanning Electron Microscope (Jeol USA, Peabody, MA, USA).

4. *In vitro* biocompatibility

4.1 Schwann cell cultures

A stabilized human neuroblastoma cell line (SH-SY5Y) was used to test *in vitro* the biological behavior of scaffolds. Cells were purchased by ECACC (European Collection of Cell Cultures, Porton Down, United Kingdom) and cultured in 75 cm^2-flasks (Corning, Milan, Italy) at a temperature of 37 °C in humidified atmosphere containing 5% CO_2. They were grown in DMEM/F-12 (1:1) basal medium (Life Technologies, Paisley, United Kingdom) added in 15% FBS (Fetal Bovine Serum, Sigma-Aldrich, Milan, Italy), 1% non-essential amino acids (Sigma-Aldrich) and 1% antibiotic solution (penicillin/streptomycin, Life technologies). At a confluence of 80-90%, SH-SY5Y were detached using 0.25% Trypsin-EDTA (Sigma-Aldrich) and reseeded for expansion. Cell lines were daily observed by optical microscope DM/IL (Leica, Wetzlar, Germany).

4.2 SH-SY5Y morphology and growth on scaffolds

After expansion, SH-SY5Y cells were detached and counted by a TC20 Automated Cell Counter (Bio-Rad). Hence, they were seeded (20,000 cells/ cm^2) on sterile disk-shaped supports made of PVA, 1 % Ox PVA and SF (prepared as previously described) and incubated at 37 °C in a 5 % CO_2 humidified atmosphere. Cell adhesion and growth on scaffolds were evaluated by SEM and 3-(4,5-dimethylthiazol-2-yl)-2,5-dimethyltetrazolium bromide (MTT) assay at 3 and 7 days after seeding.

4.2.1 SEM analysis

Briefly, at each end-point, samples were fixed for 24 h in 2.5 % glutaraldehyde in 0.1 M cacodylate buffer (pH 7.2) and dehydrated with a graded ethanol series. Thereafter, critical-point drying and gold sputtering were performed and finally samples were observed by SEM.

4.2.2 MTT assay

Proliferative activity of cells seeded on scaffolds was measured by MTT. MTT is a yellowish solution which is converted to water-insoluble MTT-formazan of purple color by mitochondrial dehydrogenases of living cells (Figure 16). The blue crystals are soluble with acidified isopropanol and the intensity can be measured colorimetrically at a wavelength of 570 nm.

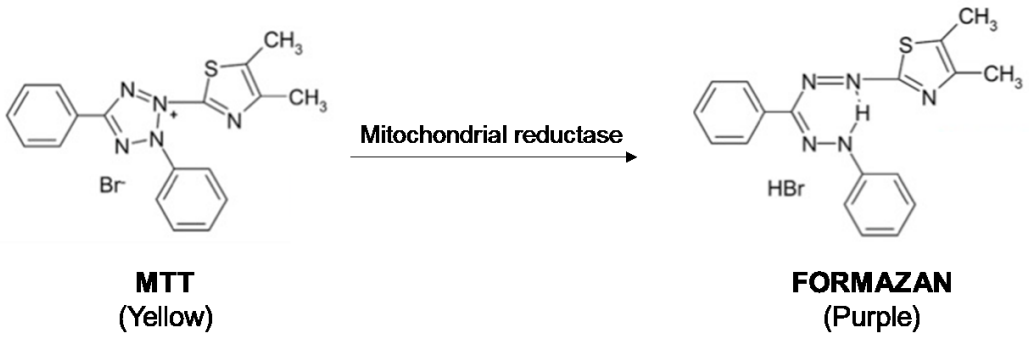

Figure 16. MTT reduction in live cells by mitochondrial reductase results in the formation of insoluble formazan, characterized by high absorptivity at 570 nm.

Hence, cell cultures were treated with a MTT solution (0.5 mg/ml) for 4 h. Formazan precipitates were solubilized in 2-propanol acid (0.04 M HCl in 2-propanol) and the optical density was measured at 570 nm using a Microplate autoreader EL 13 (BIO-TEK Instruments, Winooski, Vt., USA). Results were expressed as the number of cells grown on the seeded surface.

5. Animal Model and *in vivo* study

5.1 Experimental groups and surgical procedure

The rat sciatic nerve has served as a common model for studies on peripheral nerve regeneration. All animal procedures were approved by the ethical committee of Padua University, in agreement with the Italian Department of Health guidelines.

Fifteen Sprague-Dawley rats, weighing approximately 200-250 g, were randomly divided into 3 Groups (5 animals/group) and anaesthetized using a binary gas mixture of isoflurane and oxygen. Hence, their dorsa were carefully shaved and properly disinfected with Betadine® (Bayer, Leverkusen, Germany) before performing a 2.5 cm incision on the left thigh. After separating the fascia and muscle groups by blunt dissection, the left sciatic nerve was exposed and transected creating a nerve gap of 5 mm between the proximal and distal stumps. PVA, 1% Ox PVA and Silk-Fibroin conduits (10 mm in length) were coaxially interposed between the stumps and then sutured to the epinurium. The incision was closed in layers using 4-0 silk sutures. The controlateral sciatic nerve was considered as control. After surgery, the animals could recover in the cage and they were treated with anti-inflammatory (Rimadil, 5 mg/kg) and antibiotic (Bytril, 5 mg/kg) therapy for 5 days. In the following period, they were housed in a temperature-controlled facility and were given laboratory rodent diet and water ad libitum. Twelve weeks after surgery, the rats were euthanized by carbon dioxide asphyxiation and the implants were excised.

5.2 Analysis of the explants

The three different nerve conduits were preliminarily analyzed for their size and integrity. Thereafter, samples were properly fixed for histological, immunohistochemical and Transmission Electron Microscope (TEM) analysis to assess axonal regeneration.

5.2.1 Gross appearance of the explants

Prior to explant, the macroscopic appearance of nerve conduits was observed at the implant site. In particular, the occurrence of dislocations of the prosthesis, the presence of any inflammatory manifestations, the formation of a fibrotic capsule in correspondence of the graft or eventual neuromas at the stumps were investigated.

5.2.2 Histological and immunohistochemical analysis

Explanted samples for histological and immunohistochemical analysis were fixed in 10% formalin in PBS, embedded in paraffin, cut into 4 μm-thick serial sections, dewaxed and rehydrated; hence, sections were stained with haematoxylin and eosin (H&E) according to routine protocols. In parallel, immunological characterization of the regenerated tissue inside the nerve conduits was carried out with the following antibodies diluted in PBS: anti-CD3 (polyclonal rabbit anti-human CD3, A 0452; Dako, Milan, Italy) diluted 1:500; anti S-100 (polyclonal rabbit anti-human S100, Z 0311; Dako) diluted 1:5000. The sections were pre-treated with Dako PT Link containing FLEX TRS High pre-heated at 65°C to allow the processes of epitope retrieval. When the FLEX TRS High reached 96 °C, the instrument maintained it for 15 min. Every section was incubated with peroxidase-blocking serum (EnVision™ FLEX Peroxidase-Blocking Reagent; Dako) for 5 min to remove unspecific bindings and for 30 min with the primary antibody. A labeled polymer (EnVision™ FLEX /HRP, Dako) for 20 min and 3,3'-diaminobenzidine (EnVision™ FLEX Substrate buffer, + DAB + Chromogen; Dako) were used in order to show the positivity of the reactions, that displays the primary antibody binding. All the sections were finally counterstained with hematoxylin (EnVision™ FLEX Hematoxylin, Dako) for 5 min to reveal the presence of nuclei, dehydrated with a decreasing scale of alcohol solutions (70%, 95%, 99%), cleared with xylene and mounted. These steps were performed at RT.

5.2.3 Transmission Electron Microscope: principles of technique

Axonal regeneration was assessed by examining the ultrastructural features of the explants by the Transmission Electron Microscope (TEM).

Transmission electron microscopy involves a high voltage beam of electrons emitted by a cathode and formed by magnetic lenses. The beam of electrons, that has been partially

transmitted through the thin specimen, carries information about the structure of the sample. The spatial variation in this information (the image) is then magnified by a series of magnetic lenses until it is recorded by hitting a fluorescent screen, photographic plate, or light sensitive sensor like CCD (charge-coupled device) camera. The image detected by the CCD may be displayed in real time on a monitor or computer (Figure 17).

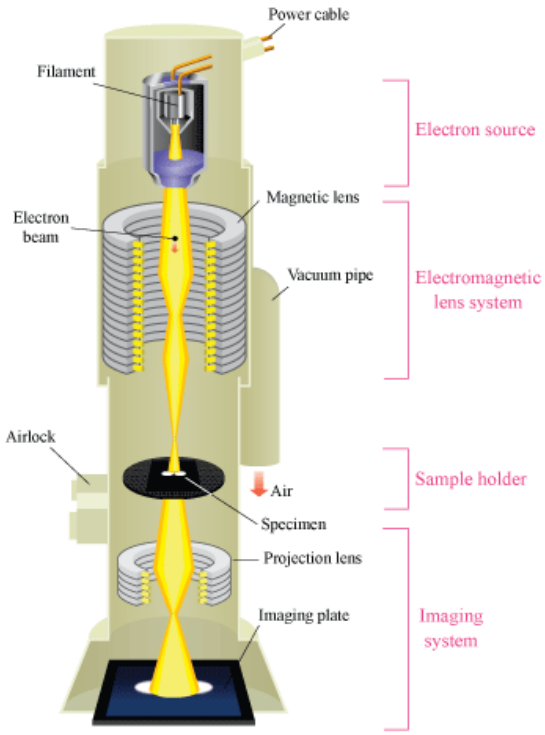

Figure 17. Transmission Electron Microscope. The transmission electron microscope consists of four parts: *a) electron source; b) electromagnetic lens system; c) sample holder; d) imaging system.* The *electron source* is an electron gun consisting in a tungsten filament which emits electrons when it is heated. Hence, through an *electromagnetic lens system* (condenser) the beam of electrons is directed on the specimen. The *sample holder* consists of a mechanical arm which holds the specimen. The *imaging system* consists of an electromagnetic lens system too and a screen which has a phosphorescent plate. The plate glows when hit by the electrons after passing through the specimen.

Preparation of the sample is an important preliminary step to the observation and it consists of three main steps: a) processing; b) embedding; c) polymerization; d) sectioning.

a) Processing

This phase includes: *fixation, rinsing, post fixation, dehydration* and *infiltration*. *Fixation* is necessary to preserve the sample and to prevent its deterioration. Glutaraldehyde is often used as fixative in TEM. Thereafter, the samples should be washed with a buffer (*rinsing)* to adjust the pH; for this purpose, sodium cacodylate buffer (pH range 5.1-7.4) is considered effective as it prevents the acidification of the specimen which may result from tissue fixation. *Post fixation* is a secondary fixation that is done using osmium tetroxide (OsO_4); it increases the stability of the sample avoiding the coagulation of many tissue proteins during dehydration by alcohols. *Dehydration* allows the replacement of tissue water with an organic solvent since the epoxy resin used in the infiltration-phase and embedding step is not miscible with water. Thereafter, the epoxy resin is used to infiltrate the sample (*infiltration*).

b) Embedding

After processing, the next step is embedding. This is done using flat molds.

c) Polymerization

During polymerization step the resin is allowed to set overnight at a temperature of 60 °C in an oven.

d) Sectioning

The specimens must be cut into sections of 30 to 60 nm in thickness using an ultramicrotome. The sections are then collected onto a copper grid and viewed under the microscope.

5.2.3.1 TEM analysis of explants

Explanted samples were fixed in 2,5% in glutaraldehyde (Serva Electrophoresis- Heidelberg-Germany) in 0.1 M phosphate buffer, post-fixed in 1% osmium tetroxide (Agar Scientific Elektron Technology - UK) in 0.1 M phosphate buffer, dehydrated in a graded alcohol series and embedded in Epoxy resin. Semi-thin sections (0.5 µm) were cut with an ultramicrotome RMC-PTX PowerTome **(**Boeckeler Instruments, Arizona-USA**)** and stained with 1% Toluidine

Blue. Images were acquired by using Leica DMR microscope.

Ultrathin sections, 60 nm, were collected on 300-mesh copper grids, counterstained with 2% uranyl acetate and then with Sato's lead. Specimens were observed by a Hitachi H-300 Transmission Electron Microscope (Japan).

5.3 Histomorphometry

The gold standard of strategies promoting peripheral nerve repair is to allow regeneration of the damaged axons, with characteristics as close as possible to the pre-injury state. In fact, one factor that influences recovery is the formation of scar tissue at the repair site, and the subsequent development of a neuroma. A common method to evaluate the quality of the regenerated nerve is to undertake histomorphometric analysis of axon types, numbers and sizes, allowing for direct measurement of axonal regeneration beyond the repair site. The ability to quantitate nerve features allows a potentially unbiased way to evaluate nerve characteristics in cases such as regrowth or pathology, and yields data less subject to variability than more subjective measures such as functional recovery (Hunter et al., 2007; Ngeow et al., 2011).

Semi-thin cross-sections obtained from the proximal, central and distal portion of explants were stained with Toluidine Blue. Thereafter, photomicrographs were acquired using a Leica DMR microscope and imported into ImageJ image processing software (National Institutes of Health, Bethesda, MD) for blinded analysis. Hence, to quantitatively compare the regenerated nerves, histomorphometric analysis of toluidine blue-stained cross sections was performed on samples. Myelinated and unmyelinated axons were observed in cross sections from the proximal, middle and distal portion of each graft. After measuring the area of each nerve, the nerve crossection was divided into 5 quadrants, and 3 highpower fields (1000x) of equal area from each quadrant were evaluated for myelinated and unmyelinated axons. Axon number was divided by the area sampled to calculate average myelinated axon density.

6. Statistical analysis

All data are expressed as means of three different experiments ± Standard Deviation (SD). Statistical significance was determined by a paired t test. Differences were considered significant with p values ≤ 0.05.

RESULTS AND DISCUSSION

1. Fabrication and morphological characterization of scaffolds

In the case of short nerve injury, the gold-standard is represented by end-to-end and fascicular suture repair techniques. However, if the nerve injury is extensive, a nerve graft is preferred to bridge the gap between the injured proximal and distal stumps (Hsiang et al., 2011). To date, Tissue Engineering is receiving an increasing attention in the treatment of peripheral nerve injuries. In fact, tissue-engineered nerve grafts may contribute in: a) creating an adequate regenerative microenvironment to guide and protect the growth of axons; b) overcoming functional donor-site defects caused by autologous nerve transplantation. In recent years, many synthetic or natural biopolymers and their composites or derivatives have been used to construct nerve scaffolds, but each has its own limitations (Xu et al., 2016).

In the present study, three different biomaterials (non-resorbable and resorbable) have been exploited with the objective of identifying from which of them can be obtain the neuro guide with the best features; after the manufacture of the scaffolds, a morphological characterization was performed first.

In Figure 18 it can be appreciated the gross appearance of disk-shaped scaffolds (A-C) and of tubular scaffolds (D-F; d-f). Considering PVA-based scaffolds, they are dimmed when they are in the shape of disks; that is highly dependent on the volume of polymer poured into the mold. Conversely, SF disk-shaped scaffolds are completely transparent.

According to SEM micrographs, PVA scaffolds showed a smooth and regular surface (Figure 19A). No porosity is visible and this aspect could be a limit; in fact, according to literature, a porous structure is useful to facilitate the transportation of the compounds needed for cell nutrition and growth and also for waste removal. Moreover, it affects the migration and organization of myofibroblasts, which are responsible for the undesired synthesis of scar tissue ([b]Arslantunali et al., 2014). Thus, a certain grade of permeability as well as the capacity to limit

and/or prevent the formation of the contractile capsule of myofibroblasts, are two key factors which must be carefully considered when working at the improvement of the tube wall properties (Cerri et al., 2014).

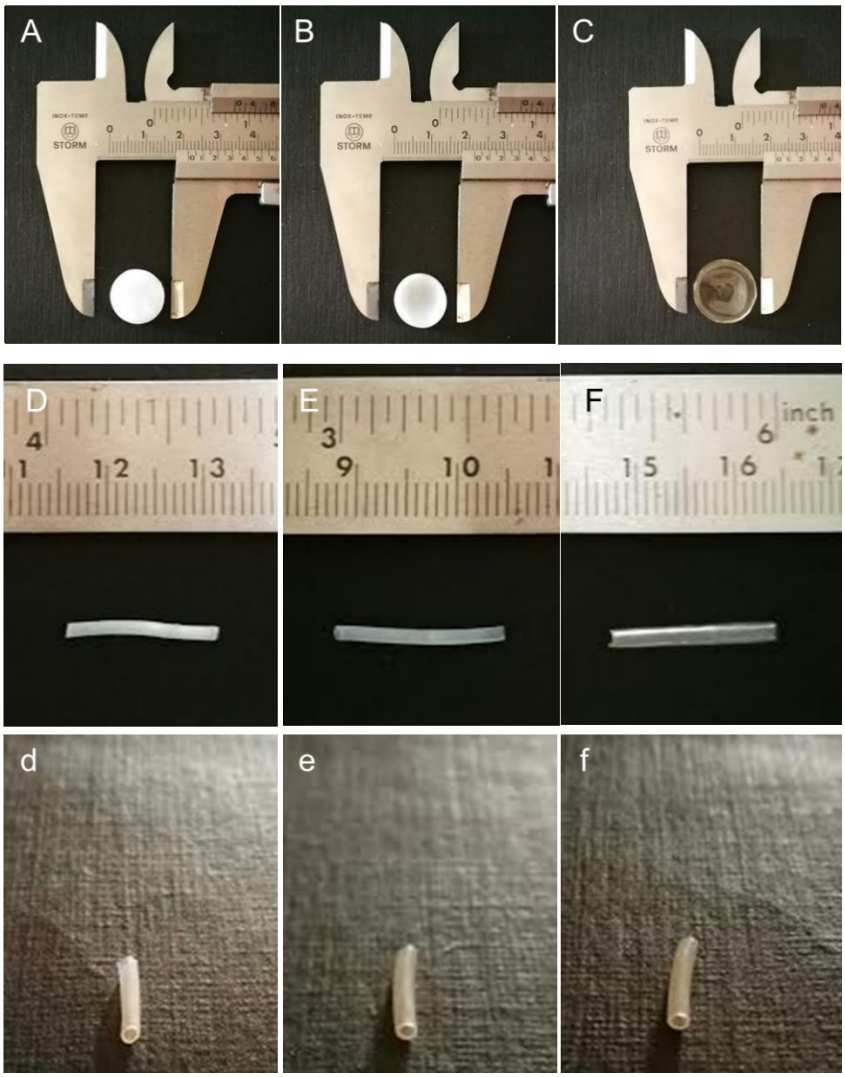

Figure 18. Gross appearance of scaffolds. Gross appearance of disk-shaped (A-C) and tubular scaffolds (D-F; d-f) made of PVA (A,D,d); 1% Ox PVA (B,E,e), SF (C,F,f).

Several studies have focused on methods that create a gradient in pore size along the tube wall. Even though an adequate porosity is considered a critical point for the enhanced nerve regeneration, conclusive results about the actual role of porous conduit to improve regeneration

in vivo are still lacking (Cerri et al., 2014).

Whereas nondegradable conduits have provided an important benchmark for nerve regeneration, their inability to degrade can result in chronic host tissue response and/or nerve compression months after implantation, deterring regeneration. Hence, to avoid these issues, biodegradable materials have been developed and utilized for the fabrication of nerve conduits regeneration (Ezra et al., 2014). In the same way, we re-engineered PVA to give the polymer such biodegradation properties. A biodegradable derivative of PVA was prepared according to a protocol we patented (Borgio et al., 2013). Briefly, through oxidation, functional groups (i.e. carbonyls) were introduced in the PVA backbone, reducing the formation of intermolecular hydrogen bonds and imparting the polymer different properties, such as lower crystallinity, faster dissolution rate and lower viscosity in aqueous milieu (Stocco et al., 2015). After cross-linking, also 1% Ox PVA hydrogels were observed by SEM. 1% Ox PVA supports have a different morphology compared to neat PVA hydrogels as they are characterized by a rough surface (Figure 19B). Hence, oxidation affects the appearance of hydrogels, likely because it influences the size of 1% Ox PVA molecules.

In parallel, another degradable biomaterial was considered. Silk fibroin is a natural polymer (unlike PVA) with great biocompatibility, mechanical properties and suitable flexibility with the ability to be used in tissue engineering (Mottaghitalab et al., 2013). Natural polymers generally suffer from batch-to-batch variance and need extensive purification and characterization; this could probably be a significant limitation in their use (Wang et Cai 2010). Several recent studies demonstrated a good potential for SF in reconstruction of peripheral nerves *in vitro* and *in vivo.* Nevertheless, despite the very promising results of these conduits, neither the FDA nor any other administration has approved any silk conduit (Gaudin et al., 2016).

As detailed previously, the disk-shaped SF scaffolds were fabricated by pouring a certain

volume of SF solution in molds. Thereafter, the solution was dried over-night and then each scaffold was incubated in 70% methanol-water. Hence, were obtained supports with a morphological appearance observable in Figure 19C. SEM micrographs highlighted a surface completely smooth. According to literature, it is possible to tune the superficial roughness and the degree of crystallinity of a fibroin film simply by varying the soaking time in a methanol solution (Servoli et al., 2005).

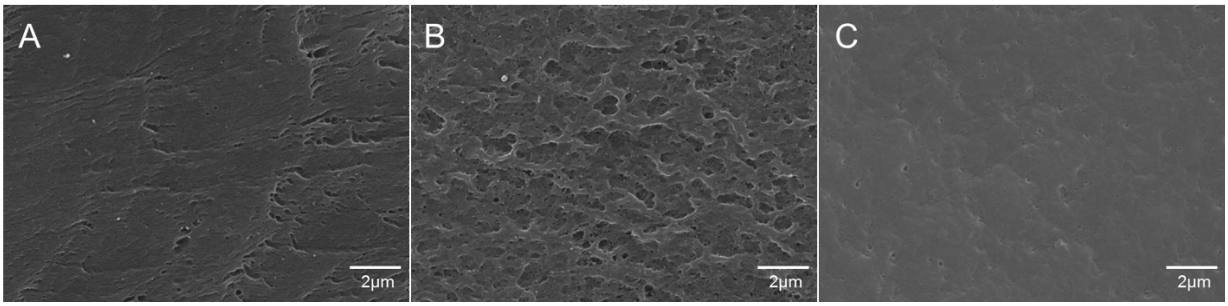

Figure 19. SEM analysis of disk-shaped scaffolds. SEM investigation of PVA(A), 1% Ox PVA (B) and SF (C) disk-shaped scaffold surface morphology.

This study allows to compare the potential of three materials, which differ in nature (natural *versus* synthetic) and intrinsic characteristics (biodegradable *versus* non-biodegradable). After a preliminary *in vitro* evaluation, the *in vivo* study will enhance the knowledge about the potential of the three biomaterials considered in promoting nerve regeneration.

2. Schwann cell growth on scaffolds

Before to develop a new nerve guide and to implant it in an animal model of peripheral nerve injury, the biomaterial must be tested for its biologic activity (cytotoxicity and biocompatibility). Once the biomaterial has proven to be non-cytotoxic and biocompatible, further studies on functional nerve repair can be conducted (Jansen et al., 2004).

In case of peripheral nerve injury, Schwann cells move from the nerve stumps towards the graft

lumen playing several important roles in nerve regeneration. *Inter alia*, they secrete neurotrophic factors (i.e. FGF, NGF, BDNF and GDNF) and express cell-adhesion molecules that promote nerve regeneration; they form the endoneurial sheath; they sustain debris clearing, creating a suitable environment for nerve growth; they myelinate axons (Heath et Rutkowski, 1998). Considered this, prior to the *in vivo* implant of PVA, 1% Ox PVA and SF nerve conduits, the biologic activity of the biomaterials was evaluated *in vitro* using a Schwann cell line (SH-SY5Y); the aim was to assess which support provides a better surface area to sustain cell adherence. Moreover, according to literature, Schwann cells seeded in nerve conduits have been successfully used for nerve reconstruction as they yield growth guidance and growth factors delivery (Gaudin et al., 2016); therefore, also this important indication may be achieved evaluating the interaction among Schwann cells and the supports.

SEM analysis and MTT assay were adopted to investigate SH-SY5Y distribution and proliferation on disk-shaped scaffolds at 3 and 7 days after seeding. According to SEM micrographs, both PVA-based scaffolds do not promote cell adhesion and proliferation as any cell was detectable on the supports at the two end-point considered (Figure 20A,B; C,D). Conversely, SF scaffolds sustain SH-SY5Y growth; as shown in Figure 20 E-H;g,h, after culturing for 3 and 7 days, cells proliferated favorably. Even though SH-SY5Y did not form a monolayer, they appeared randomly distributed on SF-scaffolds with a typical spindle-elongated morphology.

MTT assay confirmed SEM analysis results (Figure 21); PVA, as well as its oxidized variant, do not sustain cell growth in comparison with SF scaffolds (**$P \leq 0.01$) which showed also a progressive increase of cell number from day 3 to day 7 (**$P \leq 0.01$). Cell growth on tissue culture-treated polystyrene plates was considered as internal proliferation control (Ctrl).

PVA-derived scaffolds inhibit cell adhesion; however, the lack of cell adhesion is not due to any cytotoxic properties of the material. In fact, PVA hydrogels are proposed for a number of

biomedical and pharmaceutical applications (i.e. heart valves, corneal implant, cartilage substitute and arterial phantoms) and among its advantages the non-toxicity stands out.

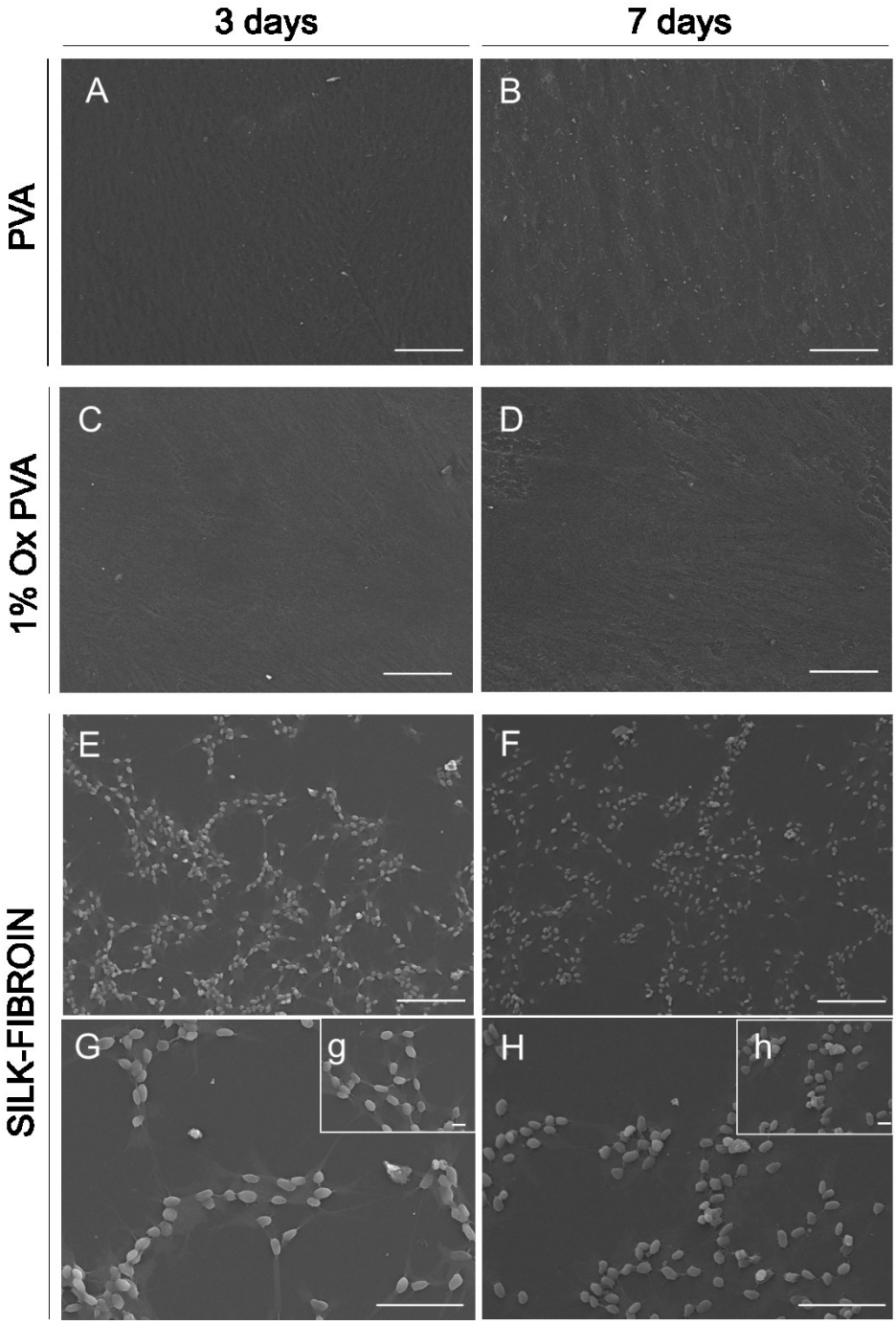

Figure 20. Assessment of cell adhesion and proliferation on scaffolds by SEM. SEM micrographs of SH-SY5Y cells after 3 and 7 days from seeding on PVA (A,B); 1% Ox PVA (C,D) and Silk-Fibroin (E-H; g,h) scaffolds. Scale bars: (A-F) 100 µm; (G,H) 50 µm; (g,h) 10 µm.

In a relevant way to certain destinations of use, cell adherence on PVA hydrogels is inhibited by its highly hydrophilic nature (Liu et al., 2010). As previously demonstrated, the same applies to the 1% Ox PVA (Stocco et al., 2014).

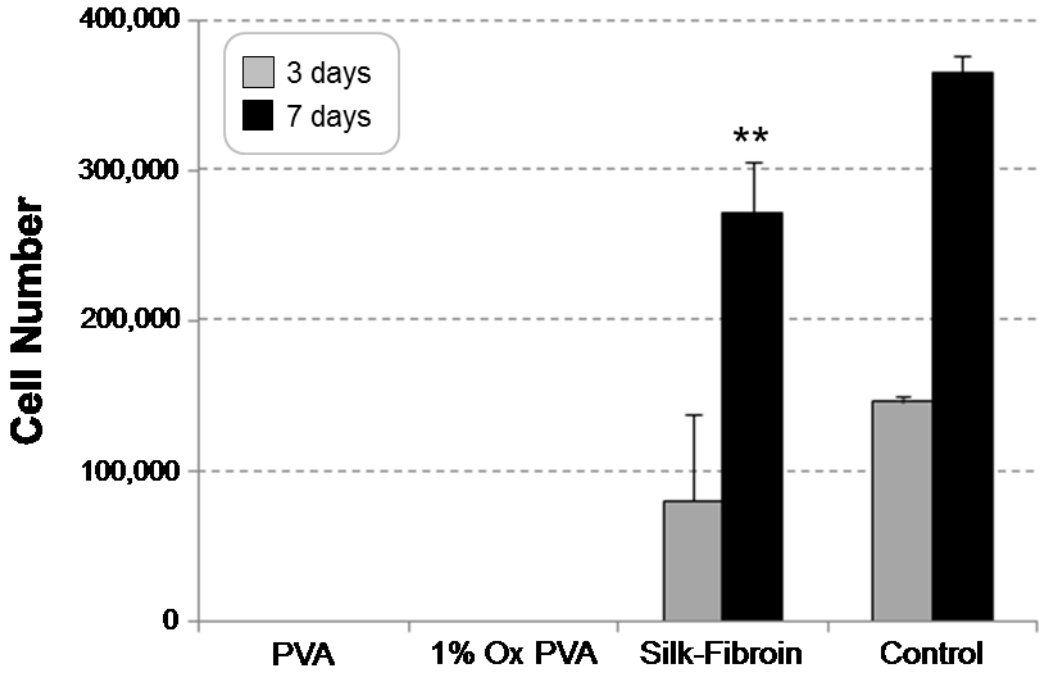

Figure 21. MTT assay. Cell growth following seeding on PVA, 1% Ox PVA and SF scaffolds. Data are average of three independent experiments ($^{**}P \leq 0.01$: Silk-Fibroin versus PVA and 1% Ox PVA; Silk-Fibroin, day 3 versus day 7).

3. Assessment of nerve regeneration *in vivo*

3.1. Nerve conduit implantation and removal

A full regeneration after nerve injury still remains one of the principle goals of regenerative biology (Gärtner et al., 2012). Considered the restrictions of current strategies, it would be beneficial for peripheral nerve regeneration to develop immediately available nerve conduits; these should match the effectiveness of autologous nerve graft, which has the limitation to be associated with a variety of clinical complications (Song et al., 2016). Thus, in this study, the

behaviour of three different synthetic scaffolds (PVA; 1% Ox PVA and Silk- Fibroin based) was evaluated.

Among non-resorbable biomaterials, PVA conduits have been approved by the US Food and Drug Administration (FDA) as the only non-degradable synthetic nerve guide (SaluBridge; SaluTunnel; SaluMedica LLC, Atlanta,GA, USA). So far, no information about the repair efficacy of these conduits has been reported in peer-reviewed journals (Gaudin et al., 2016). Considering that, the aim of this work acquires an important significance since it will allow to obtain further information about the *in vivo* use of this synthetic guide.

All animals involved in the experimental study tolerated the anesthesia/surgery and survived until the end of the observation period. Moreover, the incisions showed no signs of infection and healed adequately approximately one week after surgery.

At the time of implantation, PVA-based nerve conduits showed certain flexibility in comparison with Silk-Fibroin scaffolds. Nevertheless, all of them were easy-suturing, demonstrating also an adequate tear-resistance feature. The transparent appearance of the guides allowed to verify that the gap left between the stumps was appropriate (Figure 22A,D,G).

Three weeks after surgery, all animals developed ulcers on the left plantar; lesions were treated with the administration of antibiotics/analgesics and healed in few days.

Considering functional movement, all animals seldom moved their operated leg soon after surgery. At 12 weeks, all of them supported their body weight on the hind leg even though animals implanted with PVA and SF nerve conduits sometimes showed spasms during the walk while not limping. On the contrary, animals implanted with 1% Ox PVA nerve conduits exhibited a normal movement. Thereafter, animals were euthanized.

During dissection, all nerve conduits were still clearly recognizable; they were encapsulated in a extremely thin fibrous tissue, highlighting that the host tissue tolerated the implanted conduits without eliciting severe foreign body reactions. Moreover, visual inspection after surgery

showed that all nerve conduits preserved their round shape as well as a uniform diameter along the entire length of the implant.

When explanted, all conduits appeared well integrated into the host tissue and no dislocation was observed; furthermore, no inflammatory reaction occurred, demonstrating that implants are biocompatible with the peripheral nerve tissues. Even neuroma formation was not observed at the proximal or distal coaptation site in any of the rats (Figure 22B,E,H). Examination by surgical microscopy of explanted tubes, confirmed that nerve regeneration occurred in all experimental Groups. The high transparency of conduits, allowed to directly see the regenerated nerve throughout the lumen of the implants appearing like a white tubular substance passing along the graft (Figure 22C, F, I). In most of the literature, the regenerative nerve fibers could not be directly appreciated because the conduits are not transparent. In those cases, the grafts must be cut open for the observation of the regenerated nerve (Luo et al., 2015). Conversely, the nerve conduits investigated can be used to "*in situ*" confirm the success of formation of regenerative nerve fiber in the rat.

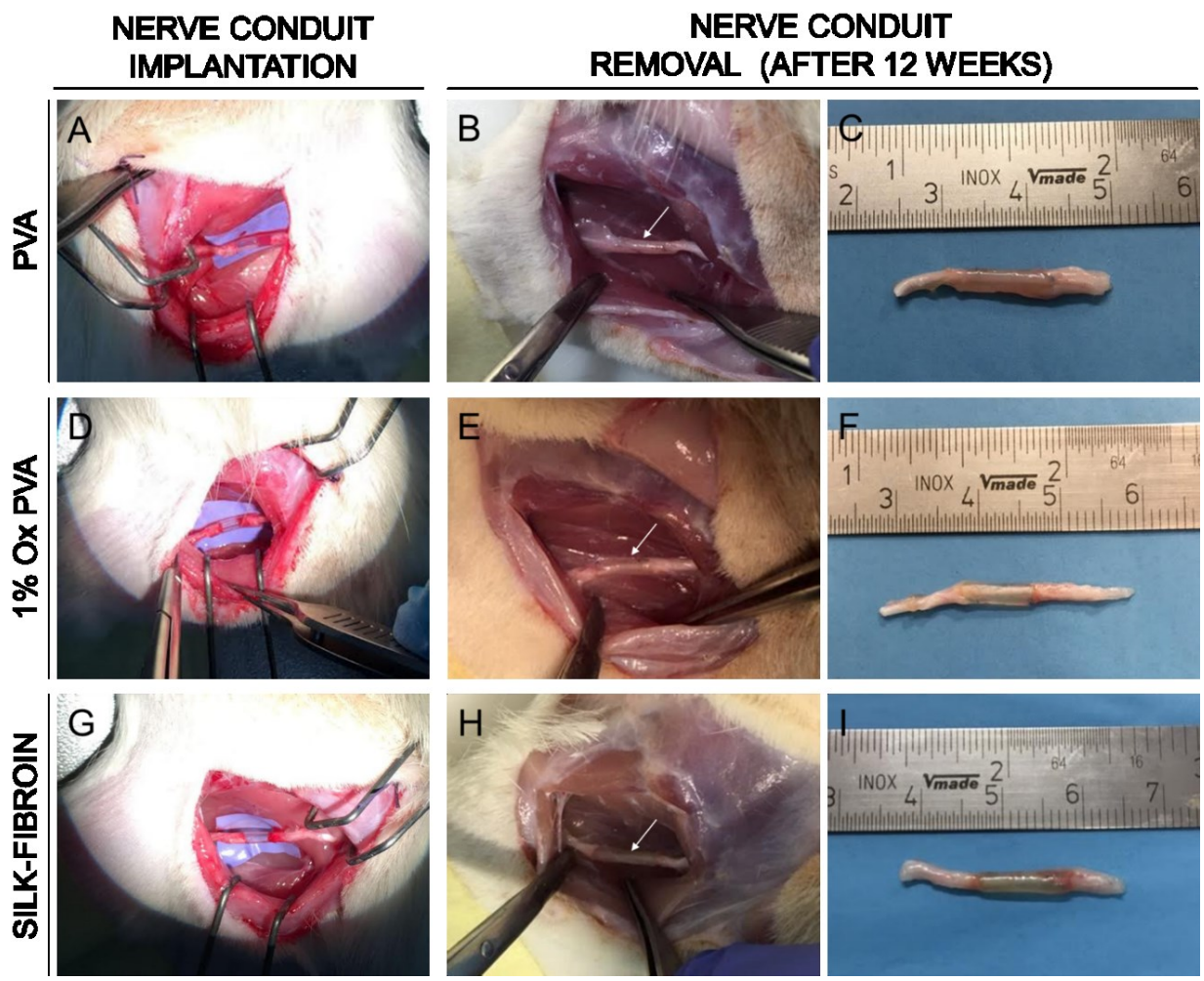

Figure 22. Nerve conduits implantation and removal. Implantation of PVA (A); 1% Ox PVA (D); Silk-Fibroin (G) nerve conduits. Twelve-weeks after surgery, the prosthesis were compared for their gross appearance at the implant site (white arrow) (B, E, H) and after the removal (C, F, I).

Ideally, a biodegradable nerve guide should be composed of a material that degrades at a rate in accordance with the rate of axonal elongation during early phases of regeneration. At this stage, the structure of the nerve guides should persist for a sufficient period to allow the formation of a fibrin matrix to connect the proximal and the distal nerve stumps. Once the initial fibrin matrix is formed, the nerve guides should degrade within a reasonable time. Otherwise, delayed nerve regeneration could happen, resulting from the compression by the guide lumen, causing epineural fibrosis thus hampering nerve regeneration and maturation (Hsiang et al., 2011). Moreover, an ideal neural scaffold should have sufficient mechanical strength to resist *in vivo* physiological loads after grafting. The animal experiments confirmed that the

mechanical properties ensure that the scaffold can resist muscular contraction and maintain its shape unchanged for a considerable period of time after grafting.

Few conduits have the properties required to an "ideal nerve guide conduit" which should be biocompatible, biodegradable, soft and flexible, semipermeable, provide a guidance cue via tubular 3D structure, prevent fibrous tissue ingrowth and meet technical requisites for sterilization, long-term storage, and surgical handling (Mottaghitalab et al., 2013). Ongoing issues, such as swelling that can occlude the inner lumen, inappropriate degradation rates, and cytotoxic degradation products, are believed to be associated with inhibiting regeneration (Ezra et al., 2014).

3.2 Axonal regeneration

Normal function of the peripheral nerve is based on morphological integrity and relationship between axons, Schwann cells, and connective sheaths, which depends on the correct development of all these components (Kaplan et al., 2009); hence, assessment of myelinated and unmyelinated nerve fiber morphology is a pillar of peripheral nerve regeneration research.

3.2.1 Istological and immunohistochemical analysis

Hematoxylin-eosin staining of the central portion of each explanted graft (PVA; 1% Ox PVA and SF) shows that the regenerated nerve successfully grew through the gap connecting proximal and distal nerve stumps (Figure 23). This finding suggests that the investigated conduits could provide correct guidance for nerve growth.

Observing Figure 23A-C, the presence of an external fibrous layer which envelopes the biomaterial is clearly identifiable; thus, proceeding toward the inside, the regenerated nerve is recognizable. Moreover, as it can be appreciated at higher magnifications (Figure 23a-c), 1% Ox PVA nerve conduit promotes the formation of a regenerated nerve characterized by a thinner

and more compact perineurium than PVA and SF guides. Anyhow, the neo-formed tissue of each section appears in the middle dense and well organized. Hematoxylin and eosin staining does not show severe inflammatory infiltrates in any sample.

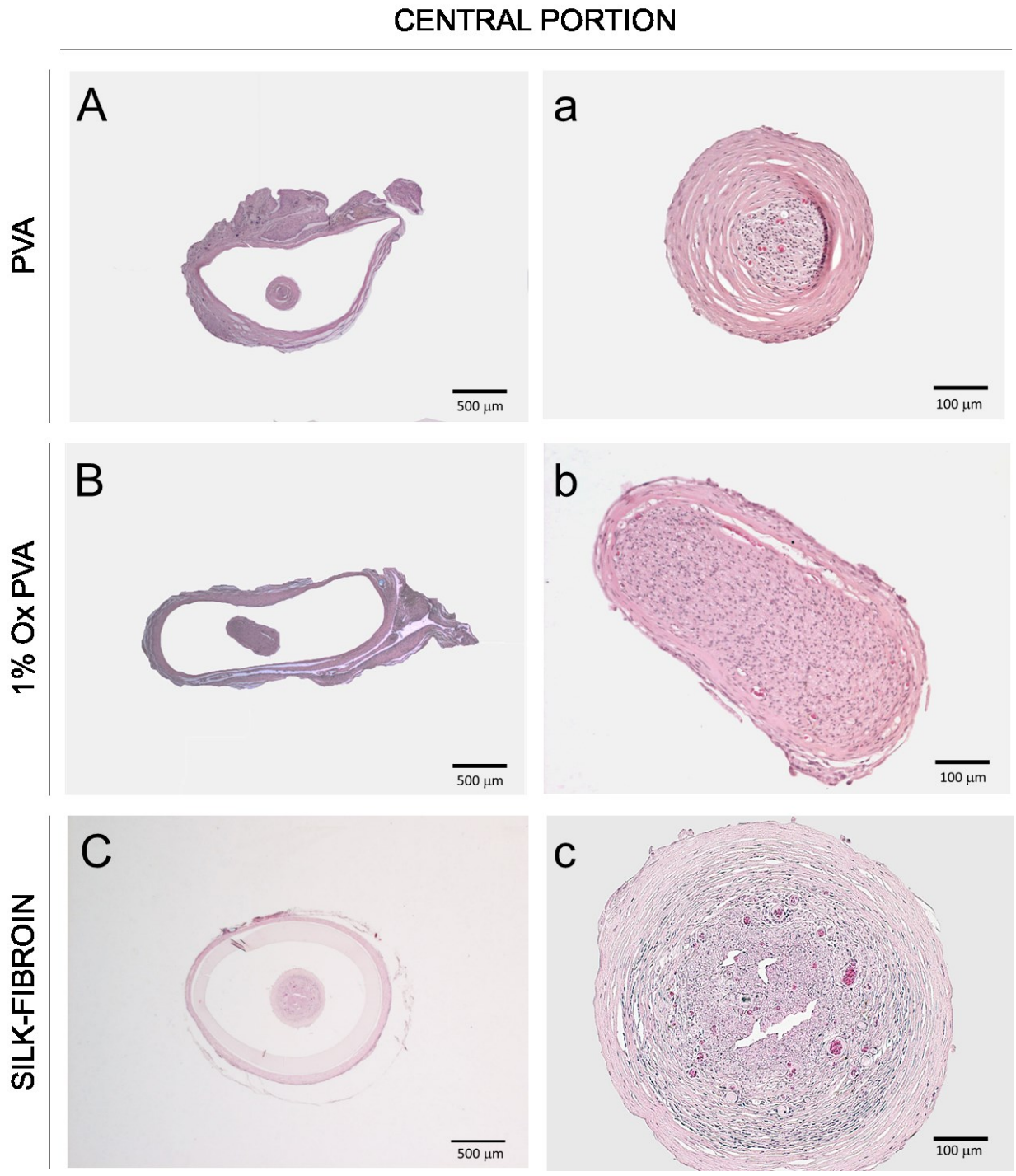

Figure 23. Hematoxylin and eosin staining of the central portion of explanted grafts. PVA (A,a); 1% Ox PVA (B,b); Silk-Fibroin (C,c).

To support the histology data, also immunohistochemical analyses were conducted.

The biocompatibility of the *grafts* was verified by evaluating the infiltration of CD3 lymphocytes. Anti-CD3 immunohistochemistry demonstrated that severe inflammatory reactions were not present in all the samples apart from a very slight infiltration of the connective tissue that surrounds the implanted material (Figure 24). These data further demonstrate that the host tissue tolerated the implanted conduits.

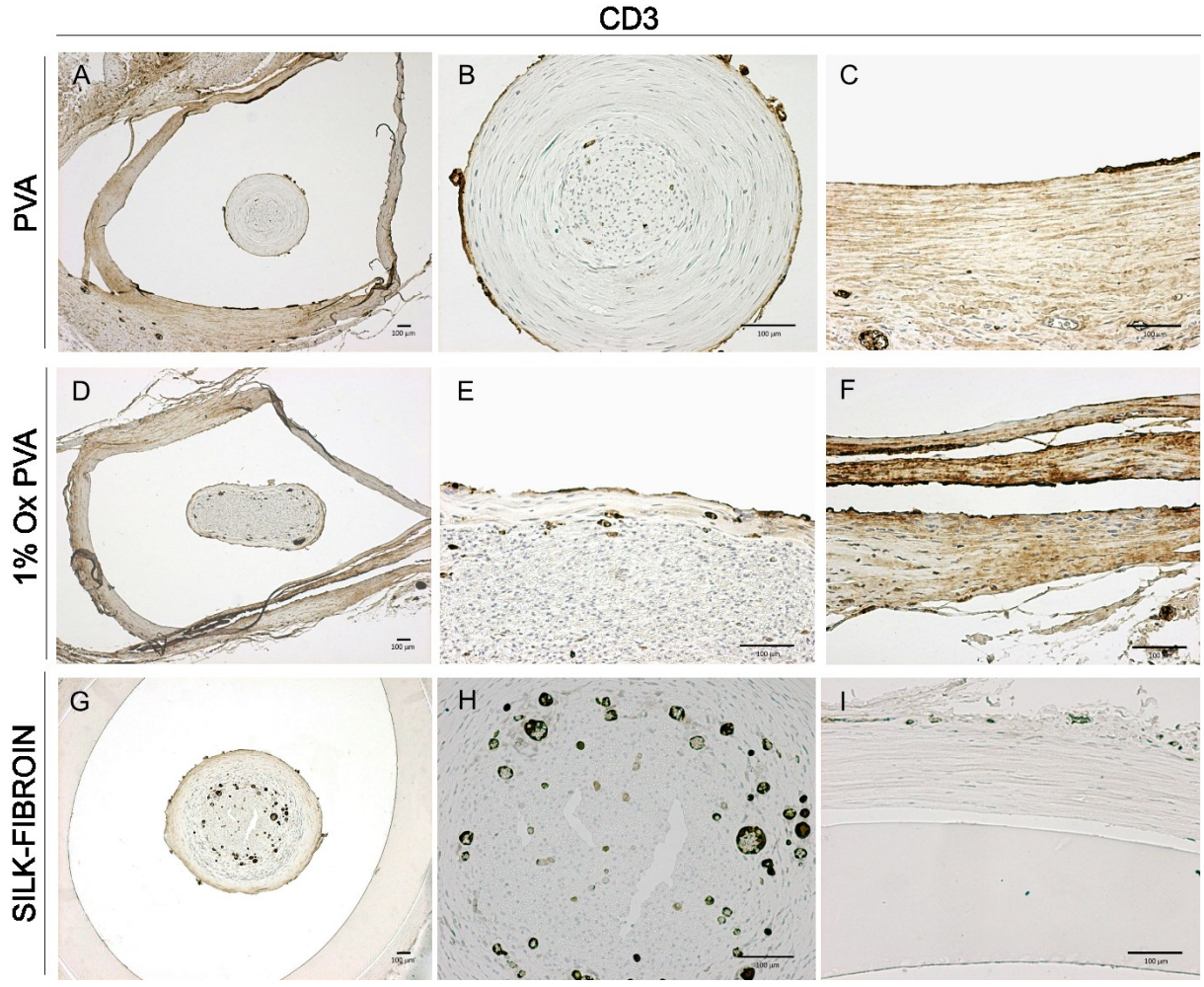

Figure 24. Immunohistochemical investigation for localization of CD3$^+$ cells on explants. PVA (A-C); 1% Ox PVA (D-F); Silk-Fibroin (G-I).

Poor functional recovery after peripheral nerve injury has been generally attributed to inability of denervated muscles to accept reinnervation and recover from denervation atrophy. However, deterioration of the Schwann cell environment may play a more vital role (Sulaiman et Gordon,

2000). Axonal regeneration within the investigated grafts was demonstrated by S100 positive staining which highlights the behavior of endogenous Schwann cells into the constructs. Schwann cells can serve as nerve guides and produce important trophic factors to stimulate axonal regeneration. An extensive endogenous Schwann cell migration into the three nerve-conduits was found, indicating the presence of regenerating axons (Figure 25).

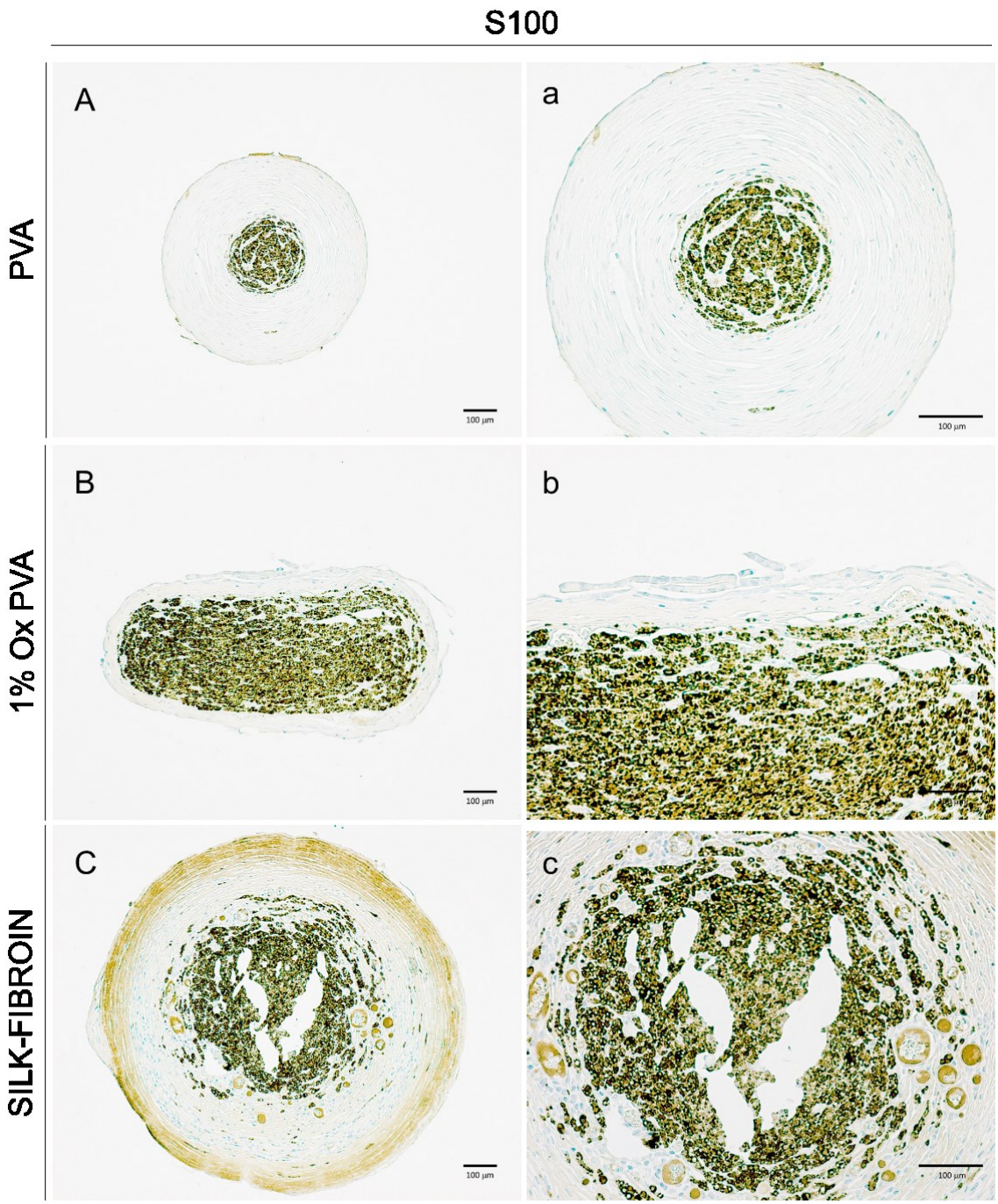

Figure 25. Immunohistochemical investigation for localization of S100^{+} cells on explants. PVA (A,a); 1% Ox PVA (B-b); Silk-Fibroin (C-c).

3.2.2 Transmission Electron Microscopy analysis

The gold standard for light microscopic imaging of nerve fibers is Toluidine Blue staining (Di Scipio et al., 2008); hence, the maturation levels of regenerated nerves were examined by comparing Toluidine Blue staining and TEM images.

Because of its peripheral nerve size, the rat sciatic nerve has been the most commonly experimental model used in this kind of studies (Gärtner et al., 2012). Figure 26 shows semithin sections Toluidine Blue-stained from the controlateral sciatic nerve of Sprague-Dawley rats (control).

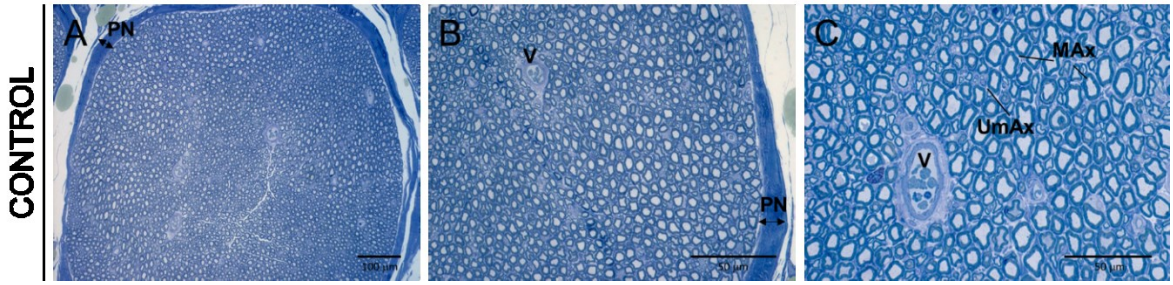

Figure 26. Native Sprague-Dawley rat sciatic nerve. Cross-sections of the sciatic nerve of a Sprague-Dawley rat stained with Toluidine Blue and considered as control. In the images are clearly identifiable the presence of: perineurium (PN); Myelinated Axons (MAx); Unmyelinated Axons (UmAx); Vessels (V).

The typical peripheral nerve morphology is clearly recognizable. Externally there is the perineurium, the connective-tissue sheath that surrounds nerve fibers. Hence, homogeneously distributed myelinated and unmyelinated axons are identifiable in the middle.

After considering the control Group, the three different scaffolds were investigated. Figure 27 refers to the central portion of explants; PVA, 1% Ox PVA and Silk-Fibroin nerve conduits are all able to support nerve regeneration, as newly-formed axons are identifiable in all sections. Nevertheless, some differences can be found between the three groups. 1% Ox PVA explants (Figure 27D-F) showed a regenerated nerve characterized by a thinner and more compact perineurium than PVA (Figure 27A-C) and Silk-Fibroin implanted animals (Figure 27G-I). In particular, Silk-Fibroin scaffolds developed the formation of a thick and fibrotic perineurium.

Also inflammatory cells are recognizable in all samples, even though the inflammatory infiltrate is clearly slighter in 1% Ox PVA conduits than the others.

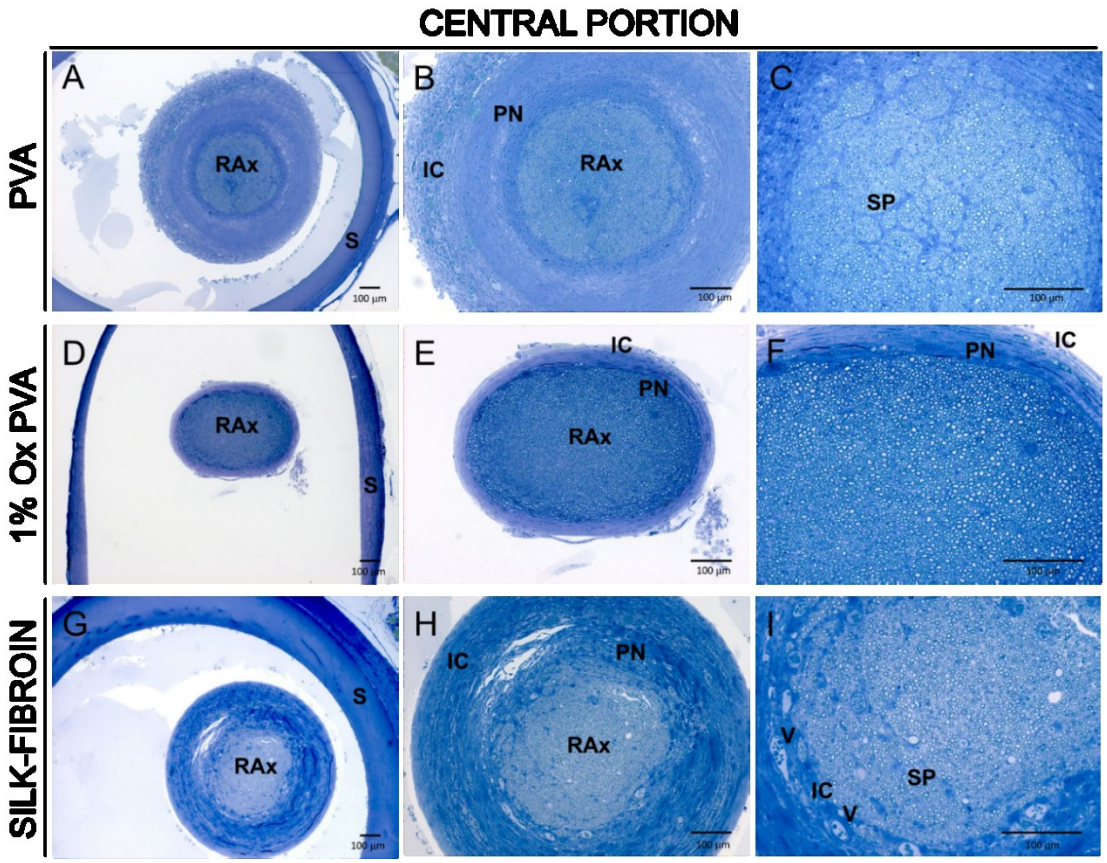

Figure 27. Evaluation of regenerated nerves at 12-weeks after surgery. Cross-sections of the central portion of: PVA (A-C); 1% Ox PVA (D-F); Silk-Fibroin (G-I) nerve conduits stained with Toluidine Blue. In the images are clearly identifiable the presence of: Scaffold (S); Regenerated Axons (RAx); Perineurium (PN); Septa (SP); Inflammatory Cells (IC); Vessels (V).

Magnifications showed in Figure 28 allows for a better assessment of the regenerated tissue quality in the central portion of the explanted nerve conduits. Many regenerated axons (myelinated and unmyelinated) are identifiable in all central sections (Figure 28B, E, H). Moreover, as it is clearly discernible, PVA and 1% Ox PVA produce a tissue regenerate characterized by compartmented myelinated and unmyelinated nerve fibers as demonstrated by the presence of septa (Figure 28B, E). This arrangement has been described as a common feature in several peripheral nerve repair procedures, including nerve autografts, and it has been accepted that it occurs in order to re-establish the endoneurial environment (Santo Neto et al.,

1998). Conversely, septa are not visible in the central portion of Silk-Fibroin nerve conduits which, on the contrary, show the presence of a fibrotic matrix surrounding axons (Figure 28H). In parallel, also the tissue-quality of proximal and the distal stumps was considered. Following axonal disruption, degenerative changes, including axon and myelin breakdown, initiate proximally and distally to the injury site. Retrograde axonal degeneration in the proximal nerve may extend for several millimeters following severe injuries and the remaining axons may also demonstrate a reduction in diameter depending on the time taken to re-establish functional connections (Deumens et al., 2010). In the distal nerve segment, Schwann cells and infiltrating macrophages participate in clearing axonal, myelin and tissue debris that follows the pattern of anterograde changes associated with Wallerian degeneration (Perry et al., 1987).

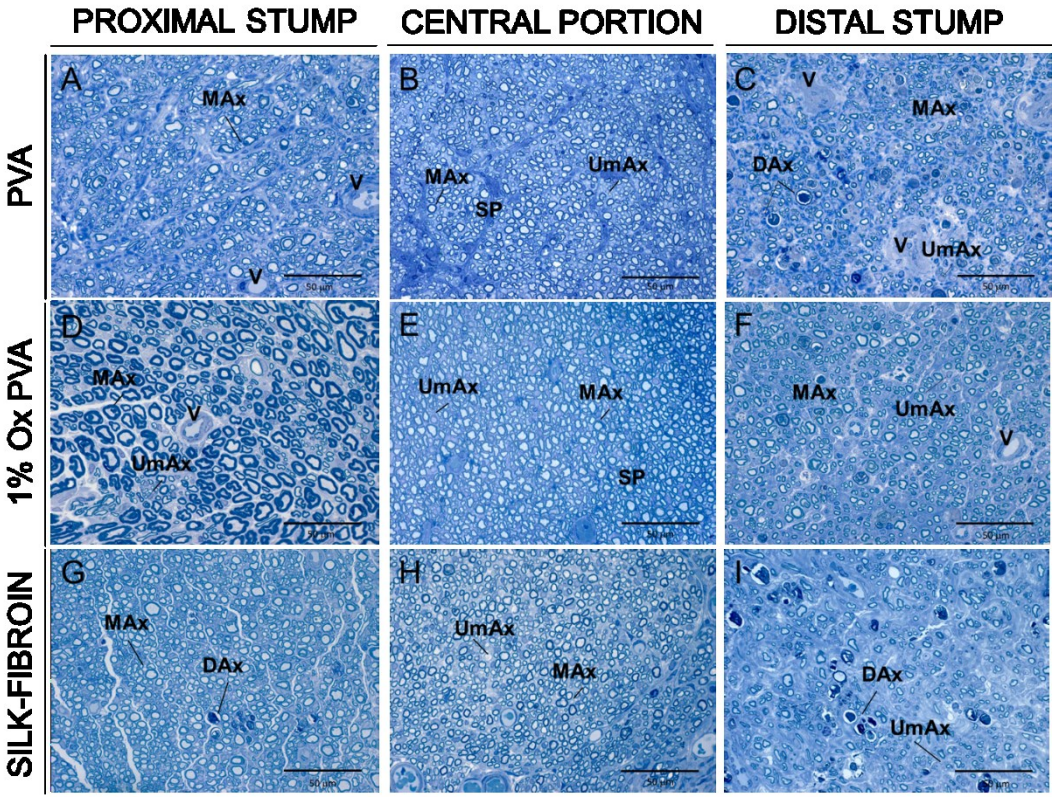

Figure 28. Assessment of nerve regeneration quality. Cross-sections of the proximal (A, D, G), central (B, E, H) and distal (C, F, I) parts of PVA (A-C), 1% Ox PVA (D-F) and Silk-Fibroin (G-I) explanted nerve conduits, stained with Toluidine Blue. In the images are clearly identifiable the presence of: Myelinated Axons (MAx); Unmyelinated Axons (UmAx); Septa (SP); Degenerated Axons (Dax); Vessels (V).

As shown in Figure 28, the proximal stump of 1 % Ox PVA samples (Figure 28D) appears different from the others (Figure 28A, G) as myelinated axons are larger and more similar to that of the control group. Many small, newly-regenerated axons are also identifiable. Degenerated axons are recognizable in the proximal and distal stump of Silk-Fibroin implanted nerves (Figure 28G, I), as well as in the distal stump of PVA-implanted samples (Figure 28C). TEM images of the central portion of explants (cross-sections) after 12-weeks surgery are showed in Figure 29. In all samples, many new-formed myelinated and unmyelinated nerve fibers are recognizable, as well as Schwann cells surrounding myelinated axons. Compared with the control group, the newly regenerated myelinated axons have a thinner myelin sheath; nevertheless the morphology of new axons is normal and adequate (Figure 29A, a).

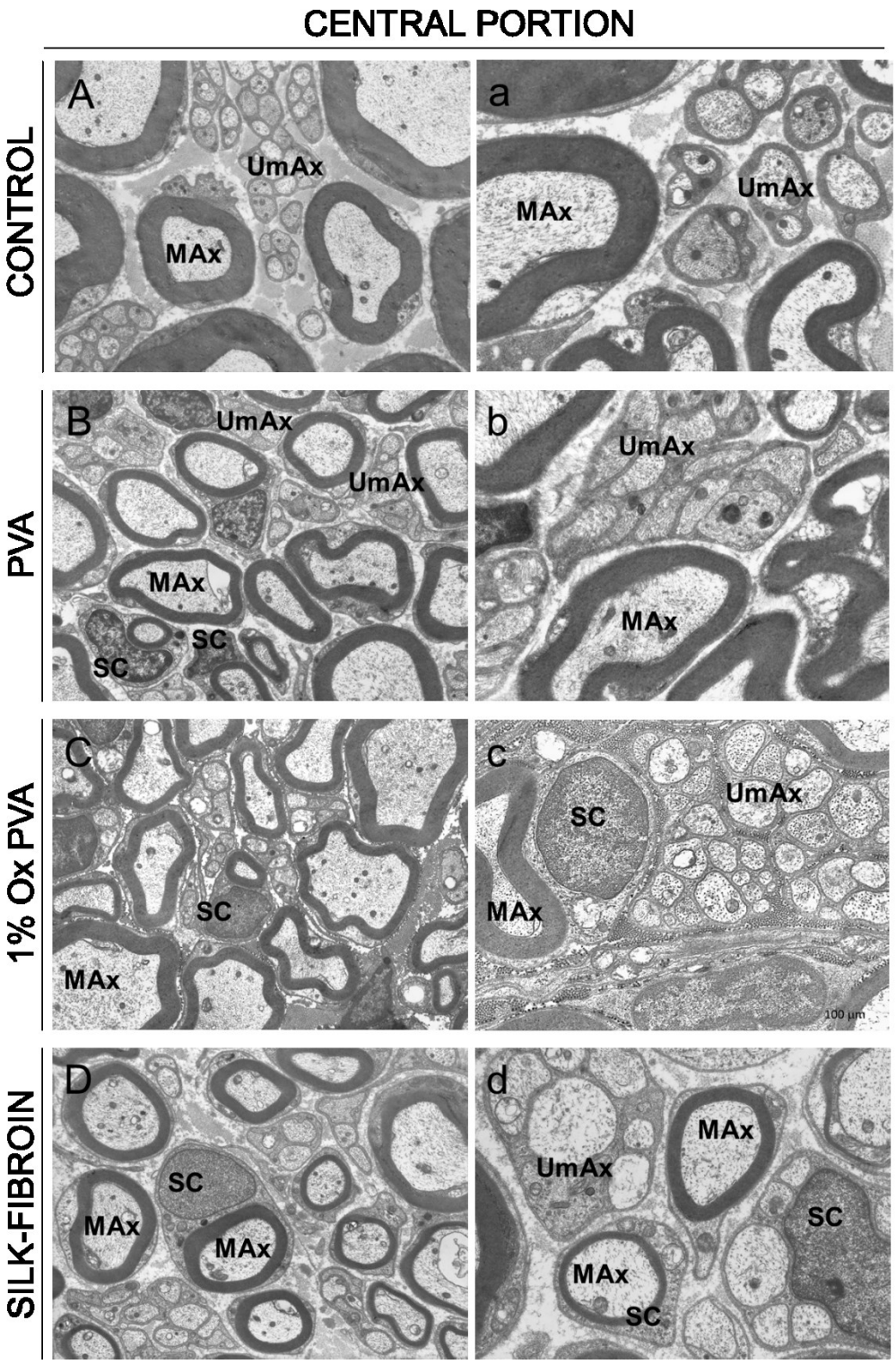

Figure 29. TEM analysis. Transverse section of the central portion of PVA (B, b); 1% Ox PVA (C, c); Silk- Fibroin (D, d) grafts in comparison with controlateral sciatic nerve considered as control (A, a). Note regenerating unmyelinated axons (UmAx) and myelinated axons (MAx) associated with Schwann cell (SC). Magnification: x 5,000 (A-D); x 10,000 (a-d).

3.2.3 Histomorphometric analysis

Quantitative histomorphometry is the current gold standard for objective measurement of nerve architecture and its components; hence, to assess axonal regeneration into the conduits a histomorphometric analysis was performed (Hunter et al., 2007).

Each specimen was divided in different portion to allow the evaluation of axonal regeneration at different levels; thus proximal (P), central (C) and distal (D) sections of each explant were considered. Controlateral sciatic nerve was used as control (Figure 30).

At first was assessed the size of the cross section of each sampling. The mean area of the control was of (543,775 μm²). Considering the explants, the measured values for each sample are reported hereinafter: PVA (P = 732,386 μm²; C = 185,599 μm²; D = 267,340 μm²); 1% Ox PVA (P = 923,492 μm²; C = 177,992 μm²; D = 305,797 μm²); Silk-Fibroin (P = 906,890 μm²; C = 210,408 μm²; D = 409,091 μm²). What seems evident is the significant difference between the cross-section area of each central portion compared to the control ($P \leq 0.01$); this can be attributed to the fact that in 12-weeks occurs the re-connection between the two stumps, nevertheless, the tissue needs more time for regenerating and become a mature nerve. Otherwise, the central portions of the three explanted samples (PVA; 1% Ox PVA; Silk-Fibroin) have comparable areas. Within the first hours following nerve transection and conduit implantation, wound fluid rich in nerve-supporting factors fills from both nerve stumps into the conduit inner lumen. During this process, the fibrin matrix accumulates naturally to form a complete bridge across the gap providing a substrate for Schwann cells migration (Ezra et al., 2014). Considering distal stumps, a reduction in size is identifiable in all the three Groups in comparison with the proximal stump. Distal Schwann cells undergo atrophy owing to the lack of contact with proximal neurons, which results in reduced expression of neurotrophic growth factors, changes in the extracellular matrix and loss of Schwann cell basal lamina, all of which hamper axonal extension. Furthermore, atrophy and denervation-related changes in target

tissues make good functional recovery difficult to achieve even when axons regenerate all the way to the target tissue (Scheib et Hake 2013).

Finally, also total axons per nerve and axon density (axons/µm²) were calculated. The measured mean values are respectively: Controlateral nerve (10,241; 0,018/µm²); PVA (P = 20,213; 0.027/µm²; C = 5,215; 0,028/µm²; D = 8,554; 0,031/µm²); 1% Ox PVA (P = 18,469; 0.020/µm²; C = 11,035; 0.062/µm²; D = 9,785; 0.032/µm²); Silk-Fibroin (P = 33,554; 0.037/µm²; C = 10,309; 0,04/µm²; D = 7,363; 0.018/µm²). The collected data suggest that 1% Ox PVA conduits assure a better outcome in nerve regeneration than the non-biodegradable PVA grafts ($P \leq 0.01$) as can be deduced by observing not only the total number of axons and the average density (axons/µm²) in section C but also comparing these values with those collected from the respective section P within each experimental Group.

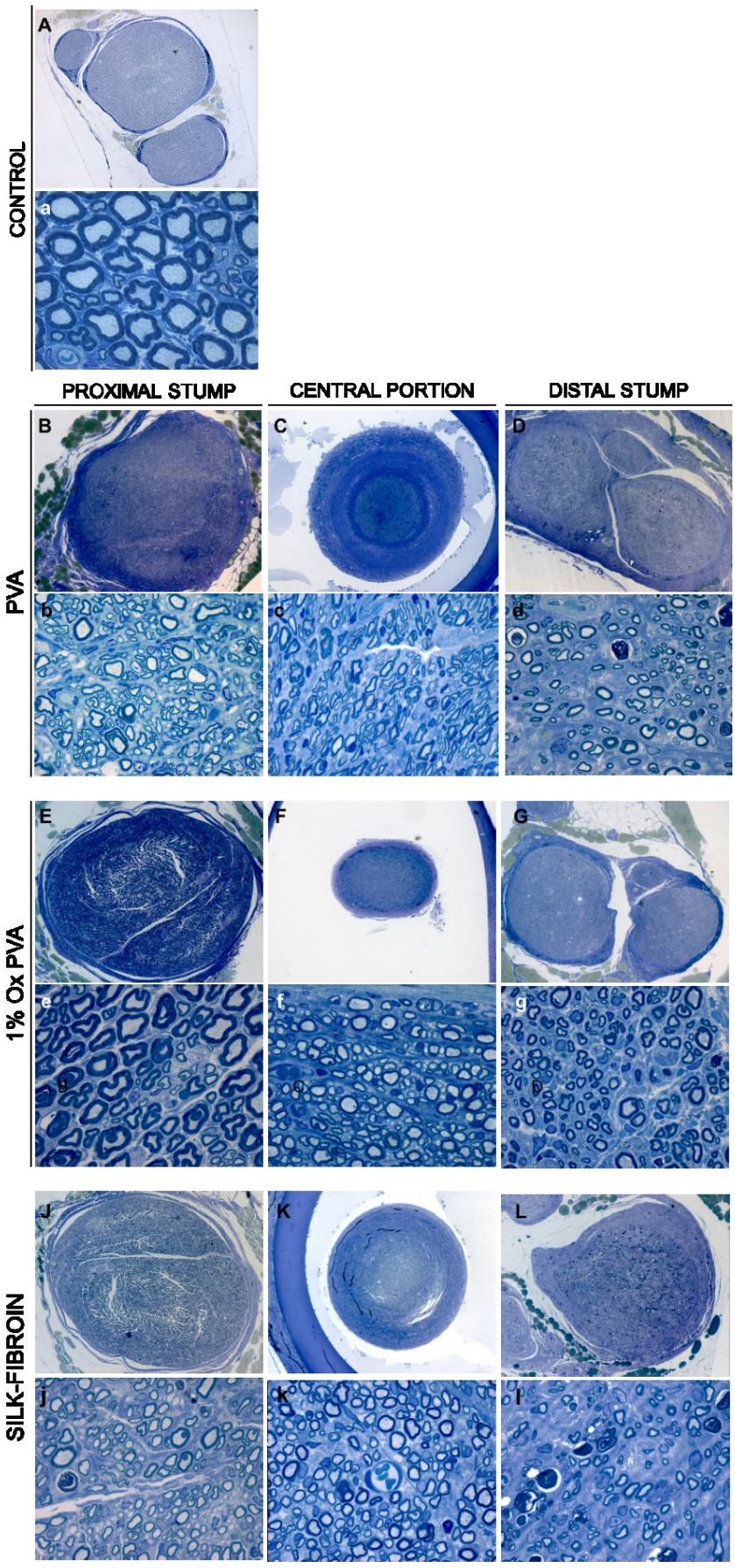

Figure 30. Representative micrographs of Toluidine-Blue-stained cross sections at different levels of the explanted grafts. Controlateral sciatic nerve (A,a); PVA (B-D;b-d); 1% Ox PVA (E-G;e-g) Silk-Fibroin (J-L; j-l).

CONCLUSIONS

In case of PNI with substance-loss, autologous nerve grafting is the treatment of choice. Nevertheless, the current challenge is to identify a device that guarantees the performance of autologous grafts (i.e. nerve grafts; vein grafts; muscle in vein grafts) without the disadvantages associated with them. Hence, the aim of this study was to investigate and compare the properties and the outcomes of three different nerve conduits in promoting peripheral nerve regeneration. The most interesting aspect concerned the different nature of the biomaterials used (PVA; 1% Ox PVA; Silk-Fibroin) as they distinguished for their origin (synthetic versus natural) and biodegradability (non-biodegradable versus biodegradable); a particular interest was aroused by the 1% Ox PVA being a material that we have patented.

According to the results of this study, all nerve conduits considered promote peripheral nerve regeneration in case of neurotmesis with loss of substance.

At 12 weeks from surgery a satisfactory functional recovery was observed in all Sprague-Dawley rats, even though a slightly better outcome was preliminary appreciated in animals implanted with 1% Ox PVA. This was afterward confirmed by Toluidine Blue staining, TEM analysis and histomorphometric analysis which quantitatively assessed axonal regeneration into the conduits.

Clinical and experimental evidences highlight the importance of absorbable tubes to overcome the limits of first-generation conduits; hence, based on the data presented, 1% Ox PVA could represent the development of the easily available and inexpensive polymer PVA. In addition to an excellent degree of manipulability during surgery due to a structure which does not collapse, elasticity and tear-resistance features, it assures nerve regenerates characterized by a homogeneous distribution of myelinated and unmyelinated nerve fibers. Moreover, it can be assumed that also the different architecture of the material (porosity) may have contributed to the obtained results.

REFERENCES

[a]Arslantunali D, Dursun T, Yucel D, Hasirci N, & Hasirci V. Peripheral nerve conduits: Technology update. Med. Devices Evid. Res. 2014; 7; 405–424.

[b]Arslantunali D, Budak G, Hasirci V. Multiwalled CNT-pHEMA composite conduit for peripheral nerve repair. J Biomed Mater Res A. 2014 Mar;102(3):828-41.

Birch R. Nerve Repair. In: Green's Operative Hand Surgery. Churchill Livingstone; 2011. 6th ed., p. 1035–1074.

Borgio L, Grandi C, Dalzoppo D. 2013; Biomateriale per dispositivi medici, in particolare protesi. Patent No.VI2013A000019, Class A61K. Deposited in 'Camera di Commercio Industria, Artigianato e Agricoltura' of Vicenza, Italy.

Cederna PS, & Chung KC. Nerve Repair and Nerve Grafting. In: Plastic Surgery: Indications and Practice. Elsevier; 2009. 1st ed., p. 1191–1199.

Cerri F, Salvatore L, Memon D, Martinelli Boneschi F, Madaghiele M, Brambilla P, Del Carro U, Taveggia C, Riva N, Trimarco A, Lopez ID, Comi G, Pluchino S, Martino G, Sannino A, Quattrini A. Peripheral nerve morphogenesis induced by scaffold micropatterning. Biomaterials. 2014 Apr;35(13):4035-45.

Chen KS, & Feldman EL. Peripheral Neuropathies. In: R. H. Winn, editor. Youmans an Winn Neurological Surgery. Elsevier; 2017. 7th ed., p. 1985–1995.e3.

Chen L, & Malessi MA. Techniques in Nerve Reconstruction and Repair. In: R. H. Winn, editor. Youmans an Winn Neurological Surgery. Elsevier; 2017. 7th ed., p. 2051–2058.e2.

Chen P, Piao X, & Bonaldo P. Role of macrophages in Wallerian degeneration and axonal regeneration after peripheral nerve injury. Acta Neuropathol. 2015.

de Ruiter GCW, Malessy MJA, Yaszemski MJ, Windebank AJ, & Spinner RJ. Designing ideal conduits for peripheral nerve repair. Neurosurg. Focus. 2009; 26(2); E5.

Deumens R, Bozkurt A, Meek MF, Marcus MA, Joosten EA, Weis J, Brook GA. Repairing injured peripheral nerves: Bridging the gap. Prog Neurobiol. 2010 Nov;92(3):245-76.

Di Scipio F1, Raimondo S, Tos P, Geuna S. A simple protocol for paraffin-embedded myelin sheath staining with osmium tetroxide for light microscope observation. Microsc Res Tech. 2008 Jul;71(7):497-502.

Dillingham T, Andary M, & Dumitru D. Electrodiagnostic Medicine. In: Braddom's Physical Medicine and Rehabilitation. Elsevier; 2016. 5th ed., p. 131–163.e12.

Drake RL, Vogl AW, & Mitchell AWM. The Body. In: Gray's Anatomy for Students. Churchill Livingstone; 2014. 3rd ed., p. 1–50.

Ezra M, Bushman J, Shreiber D, Schachner M, Kohn J. Enhanced femoral nerve regeneration after tubulization with a tyrosine-derived polycarbonate terpolymer: effects of protein adsorption and independence of conduit porosity. Tissue Eng Part A. 2014 Feb;20(3-4):518-28.

Felten DL, O'Banion MK, & Maida MS. Peripheral Nervous System. In: Netter's Atlas of Neuroscience. Elsevier; 2016. 3rd ed., p. 153–231.

Gärtner A, Pereira T, Simões MJ, Armada-da-Silva PA, França ML, Sousa R, Bompasso S, Raimondo S, Shirosaki Y, Nakamura Y, Hayakawa S, Osakah A, Porto B, Luís AL, Varejão AS, Maurício AC. Use of hybrid chitosan membranes and human mesenchymal stem cells from the Wharton jelly of umbilical cord for promoting nerve regeneration in an axonotmesis rat model. Neural Regen Res. 2012 Oct 15;7(29):2247-58.

Gaudin R, Knipfer C, Henningsen A, Smeets R, Heiland M, & Hadlock T. Approaches to peripheral nerve repair: Generations of biomaterial conduits yielding to replacing autologous nerve grafts in craniomaxillofacial surgery. Biomed Res. Int. 2016.

Gaudin R, Knipfer C, Henningsen A, Smeets R, Heiland M, Hadlock T. Approaches to Peripheral Nerve Repair: Generations of Biomaterial Conduits Yielding to Replacing Autologous Nerve Grafts in Craniomaxillofacial Surgery.Biomed Res Int. 2016;2016:3856262.

Goonoo N, Bhaw-Luximon A, Passanha P, Esteves SR, & Jhurry D. Third generation poly(hydroxyacid) composite scaffolds for tissue engineering. J. Biomed. Mater. Res. - Part B Appl. Biomater. 2016.

Grinsell D, & Keating CP. Peripheral Nerve Reconstruction after Injury : A Review of Clinical and Experimental Therapies. J. BioMed Res. Int. 2014; 2014; 698256.

Gu X, Ding F, Williams DF. Neural tissue engineering options for peripheral nerve regeneration. Biomaterials. 2014 Aug;35(24):6143-56.

Gu X, Ding F, Yang Y, & Liu J. Construction of tissue engineered nerve grafts and their application in peripheral nerve regeneration. Prog. Neurobiol. 2011.

Heath CA, Rutkowski GE. The development of bioartificial nerve grafts for peripheral-nerve regeneration. Trends Biotechnol. 1998 Apr;16(4):163-8.

Hebert-Blouin M-N, & Spinner RJ. Nerve Injury and Repair. In: Current Surgical Therapy. Elsevier; 2017. 12th ed., p. 850–858.

Hsiang SW, Tsai CC, Tsai FJ, Ho TY, Yao CH, Chen YS.. Novel use of biodegradable casein conduits for guided peripheral nerve regeneration. J R Soc Interface. 2011 Nov 7;8(64):1622-34

Huang W, Begum R, Barber T, Ibba V, Tee NCH, Hussain M, Arastoo M, Yang Q, Robson LG, Lesage S, Gheysens T, Skaer NJ V, Knight DP, & Priestley J V. Regenerative potential of silk conduits in repair of peripheral nerve injury in adult rats. Biomaterials. 2012; 33(1); 59–71.

Hunter DA, Moradzadeh A, Whitlock EL, Brenner MJ, Myckatyn TM, Wei CH, Tung TH, Mackinnon SE. Binary imaging analysis for comprehensive quantitative histomorphometry of peripheral nerve. J Neurosci Methods. 2007 Oct 15;166(1):116-24.

Jansen K, van der Werff JF, van Wachem PB, Nicolai JP, de Leij LF, van Luyn MJ. A hyaluronan-based nerve guide: in vitro cytotoxicity, subcutaneous tissue reactions, and degradation in the rat. Biomaterials. 2004 Feb;25(3):483-9.

Jobe MT, & Martinez SF. Peripheral Nerve Injuries. In: F. Azar, T. S. Canale, & J. Beaty, editors. Campbell's Operative Orthopaedics. Elsevier; 2016. 13th ed., p. 3062–3127.

Jobe MT. Nerve Injuries. In: Campbell's Operative Orthopaedics. Elsevier; 2017. 13th ed., p. 3462–3477.e2.

Kaplan S, Odaci E, Unal B, Sahin B, Fornaro M. Chapter 2: Development of the peripheral nerve. Int Rev Neurobiol. 2009;87:9-26.

Kelly EJ, Jacoby C, Terenghi G, Mennen U, Ljungberg C, & Wiberg M. End-to-side nerve coaptation: a qualitative and quantitative assessment in the primate. J. Plast. Reconstr. Aesthet. Surg. 2007, Jan 1; 60(1); 1–12.

Kim TH, An DB, Oh SH, Kang MK, Song HH, Lee JH. Creating stiffness gradient polyvinyl alcohol hydrogel using a simple gradual freezing-thawing method to investigate stem cell differentiation behaviors. Biomaterials 2015; 40:51-60.

Kwei SL, Weiss DD, & Pribaz J. Microsurgery and Free Flaps. In: Plastic Surgery: Indications and Practice. Elsevier; 2009. 1st ed., p. 79–94.

Liu Y, Geever LM, Kennedy JE, Higginbotham CL, Cahill PA, McGuinness GB. Thermal behavior and mechanical properties of physically crosslinked PVA/Gelatin hydrogels. J Mech Behav Biomed Mater. 2010 Feb;3(2):203-9.

Luo L, Gan L, Liu Y, Tian W, Tong Z, Wang X, Huselstein C, Chen Y. Construction of nerve guide conduits from cellulose/soy protein composite membranes combined with Schwann cells and pyrroloquinoline quinone for the repair of peripheral nerve defect. Biochem Biophys Res Commun. 2015 Feb 20;457(4):507-13.

Malik AF, Hoque R, Ouyang X, Ghani A, Hong E, Khan K, Moore LB, Ng G, Munro F, Flavell RA, Shi Y, Kyriakides TR, & Mehal WZ. Inflammasome components Asc and caspase-1 mediate biomaterial-induced inflammation and foreign body response. Proc. Natl. Acad. Sci. 2011, Dec 13; 108(50); 20095–20100.

Meek MF, & Coert JH. US Food and Drug Administration /Conformit Europe- approved absorbable nerve conduits for clinical repair of peripheral and cranial nerves. Ann Plast Surg. 2008; 60(1); 466–472.

Millesi H. Peripheral nerve injuries. Nerve sutures and nerve grafting. Scand. J. Plast. Reconstr. Surg. - Suppl. 1982; 19; 25–37.

Millesi H. Techniques for nerve grafting. Hand Clin. 2000; 16(1); 73–91, viii.

Mohammadi J, Delaviz H, Mohammadi B, Delaviz H, Rad P. Comparison of repair of peripheral nerve transection in predegenerated muscle with and without a vein graft. BMC Neurol. 2016 Nov 22;16(1):237.

Mottaghitalab F, Farokhi M, Zaminy A, Kokabi M, Soleimani M, Mirahmadi F, Shokrgozar MA, Sadeghizadeh M. A biosynthetic nerve guide conduit based on silk/SWNT/fibronectin nanocomposite for peripheral nerve regeneration. PLoS One. 2013 Sep 30;8(9):e74417.

Ngeow WC, Atkins S, Morgan CR, Metcalfe AD, Boissonade FM, Loescher AR, Robinson PP. Histomorphometric changes in repaired mouse sciatic nerves are unaffected by the application of a scar-reducing agent. J Anat. 2011 Nov;219(5):638-45.

Pabari A, Lloyd-Hughes H, Seifalian AM, & Mosahebi A. Nerve conduits for peripheral nerve surgery. Plast. Reconstr. Surg. 2014; 133(6); 1420–30.

Pancrazio JJ, Wang F, & Kelley CA. Enabling tools for tissue engineering. Biosens. Bioelectron. 2007.

Park SY, Ki CS, Park YH, Lee KG, Kang SW, Kweon HY, & Kim HJ. Functional recovery guided by an electrospun silk fibroin conduit after sciatic nerve injury in rats. J. Tissue Eng. Regen. Med. 2015; 9(1); 66–76.

Perry VH, Brown MC, Gordon S. The macrophage response to central and peripheral nerve injury. A possible role for macrophages in regeneration. J Exp Med. 1987 Apr 1;165(4):1218-23.

Ringkamp M, Raja SN, Campbell JN, & Meyer R. Peripheral Mechanisms of Cutaneous Nociception. In: Wall & Melzack's Textbook of Pain. Elsevier; 2013. 6th ed., p. 1–30.

Roberts CS, Seligson D, & Hartley B. Diagnosis and Treatment of Complications. In: Skeletal Trauma: Basic Science, Management and Reconstruction. Elsevier; 2015. 5th ed., p. 579–608.e7.

Rockwood DN, Preda RC, Yücel T, Wang X, Lovett ML, Kaplan DL. Materials fabrication from Bombyx mori silk fibroin. Nat Protoc. 2011 Sep 22;6(10):1612-31.

Rubin LG, & Papsin B. Cochlear implants in children: surgical site infections and prevention and treatment of acute otitis media and meningitis. Pediatrics. 2010; 126(2); 381–391.

Rutkowski GE, & Heath CA. Development of a bioartificial nerve graft. II. Nerve regeneration in vitro. Biotechnol. Prog. 2002; 18(2); 373–379.

Santo Neto H, Teodori RM, Somazz MC, Marques MJ. Axonal regeneration through muscle autografts submitted to local anaesthetic pretreatment. Br J Plast Surg. 1998 Oct;51(7):555-60.

Scheib J, Höke A. Advances in peripheral nerve regeneration. Nat Rev Neurol. 2013 Dec;9(12):668-76.

Servoli E, Maniglio D, Motta A, Predazzer R, Migliaresi C. Surface properties of silk fibroin films and their interaction with fibroblasts. Macromol Biosci. 2005 Dec 15;5(12):1175-83.

Shi Y, Zhou L, Tian J, & Wang Y. Transplantation of neural stem cells overexpressing glia-derived neurotrophic factor promotes facial nerve regeneration. Acta Otolaryngol. 2009; 129(8); 906–914.

Siemionow M, Bozkurt M, & Zor F. Regeneration and repair of peripheral nerves with different biomaterials: review. Microsurgery. 2010, Oct; 30(7); 574–88.

Siemionow M, Bozkurt M, Zor F. Regeneration and repair of peripheral nerves with different biomaterials: review. Microsurgery. 2010 Oct;30(7):574-88.

Sinis N, Kraus A, Papagiannoulis N, Werdin F, Schittenhelm J, Meyermann R, Haerle M, Geuna S, & Schaller H-E. Concepts and Developments in Peripheral Nerve Surgery. Clin. Neuropathol. 2009; 28(4); 247–262.

Sonabend AM, Smith P, Huang JH, & Winfree C. Peripheral Nerve Injury. In: Schmidek & Sweet's Operative Neurosurgical Techniques. Saunders; 2012. 6th ed., p. 2225–2238.

Song J, Sun B, Liu S, Chen W, Zhang Y, Wang C, Mo X, Che J, Ouyang Y, Yuan W, Fan C. Polymerizing Pyrrole Coated Poly (l-lactic acid-co-ε-caprolactone) (PLCL) Conductive Nanofibrous Conduit Combined with Electric Stimulation for Long-Range Peripheral Nerve Regeneration. Front Mol Neurosci. 2016 Nov 8;9:117.

Spiller KL, Maher SA, Lowman AM. Hydrogels for the repair of articular cartilage defects. Tissue Eng Part B Rev 2011; 17(4):281-99.

Squintani G, Bonetti B, Paolin A, Vici D, Cogliati E, Murer B, & Stevanato G. Nerve regeneration across cryopreserved allografts from cadaveric donors: a novel approach for peripheral nerve reconstruction. J. Neurosurg. 2013; 119(4); 907–13.

Stocco E, Barbon S, Dalzoppo D, Lora S, Sartore L, Folin M, Parnigotto PP, Grandi C. Tailored PVA/ECM scaffolds for cartilage regeneration. Biomed Res Int. 2014;2014:762189.

Stocco E, Barbon S, Grandi F, Gamba PG, Borgio L, Del Gaudio C, Dalzoppo D, Lora S, Rajendran S, Porzionato A, Macchi V, Rambaldo A, De Caro R, Parnigotto PP, Grandi C. Partially oxidized polyvinyl alcohol as a promising material for tissue engineering. J Tissue Eng Regen Med. 2015 Oct 29. doi: 10.1002/term.2101. [Epub ahead of print].

Sulaiman OA, Gordon T. Effects of short- and long-term Schwann cell denervation on peripheral nerve regeneration, myelination, and size. Glia. 2000 Dec;32(3):234-46.

Trapp BD, & Herrup K. Neurons and Neuroglia. In: R. H. Winn, editor. Youmans an Winn Neurological Surgery2. Elsevier; 2017. 7th ed., p. e326–e346.

Tsao B, Boulis N, & Murray B. Trauma of the Nervous System: Peripheral Nerve Trauma. In: Bradley's Neurology in Clinical Practice. Elsevier; 2016. 7th ed., p. 903–919.e2.

Wang S, & Cai L. Polymers for fabricating nerve conduits. Int. J. Polym. Sci. 2010.

Wang S, Cai L. Polymers for Fabricating Nerve Conduits. Int. J of Polymer Sci. Volume 2010, Article ID 138686, 20 pages, doi:10.1155/2010/138686.

Wang X, Pan M, Wen J, Tang Y, Hamilton AD, Li Y, Qian C, Liu Z, Wu W, & Guo J. A novel artificial nerve graft for repairing long-distance sciatic nerve defects: a self-assembling peptide nanofiber scaffold-containing poly(lactic-co-glycolic acid) conduit. Neural Regen. Res. 2014, Dec 15; 9(24); 2132–2141.

Weber R V., & Mackinnon SE. Peripheral Nerve Injuries. In: Plastic Surgery Secrets Plus. Mosby; 2010. 2nd ed., p. 880–886.

Xu Y, Zhang Z, Chen X, Li R, Li D, Feng S.A Silk Fibroin/Collagen Nerve Scaffold Seeded with a Co-Culture of Schwann Cells and Adipose-Derived Stem Cells for Sciatic Nerve Regeneration. PLoS One. 2016 Jan 22;11(1):e0147184.